NISTIR 6027

THE THERMAL RESPONSE OF GYPSUM-PANEL/STEEL-STUD WALL SYSTEMS EXPOSED TO FIRE ENVIRONMENTS - A SIMULATION FOR USE IN ZONE-TYPE FIRE MODELS

Leonard Y. Cooper

United States Department of Commerce
Technology Administration
National Institute of Standards and Technology

NISTIR 6027

THE THERMAL RESPONSE OF GYPSUM-PANEL/STEEL-STUD WALL SYSTEMS EXPOSED TO FIRE ENVIRONMENTS - A SIMULATION FOR USE IN ZONE-TYPE FIRE MODELS

Leonard Y. Cooper

June 1997
Building and Fire Research Laboratory
National Institute of Standards and Technology
Gaithersburg, MD 20899

U.S. Department of Commerce
William M. Daley, *Secretary*
Technology Administration
Gary R. Bachula, *Acting Under Secretary for Technology*
National Institute of Standards and Technology
Robert E. Hebner, *Acting Director*

TABLE OF CONTENTS

LIST OF TABLES AND FIGURES

Page

THE THERMAL RESPONSE OF GYPSUM-PANEL/STEEL-STUD WALL SYSTEMS EXPOSED TO FIRE ENVIRONMENTS - A SIMULATION FOR USE IN ZONE-TYPE FIRE MODELS

Leonard Y. Cooper

ABSTRACT

This work develops a method for simulating the thermal response of fire-environment-exposed wall systems constructed of arbitrary-thickness gypsum panels mounted on either side of vertical steel studs. The studs, separated at regular intervals, form an unfilled air gap between the panels

The main objective is an experimentally-validated, modular, thermal-wall-model algorithm that can be easily integrated into zone-type compartment fire models and that can be used in "stand-alone" analyses.

The algorithm solves an initial-value/boundary-value problem for the temperature distribution through the thicknessess of the two panels and within a specified time interval. The analysis is based on temperature-dependent thermal properties for the gypsum. The initial temperature distribution and the type of boundary conditions at the outer surfaces are user-specified. A variety of choices for the boundary conditions are available. These include boundary conditions that are expected to satisfy the requirements of any zone-type fire model and those that can be used to determine fire performance of the wall systems in ASTM E119 or ISO 834 tests. The algorithm output includes the final temperature distribution and, when outer surface temperatures are specified, the final rate of heat transfer to these surfaces.

Keywords: **Algorithms, ASTM E119, compartment fires, fire barriers, fire models, gypsum board, steel studs, walls, zone models**

INTRODUCTION - THE WALL SYSTEM AND BASIC ELEMENTS OF A THERMAL MODEL

The purpose of this work is to develop a method for simulating the thermal response of wall systems constructed of gypsum panels mounted on steel studs to fire environment exposures. The main objective is an experimentally-verified, modular, thermal-wall-model algorithm that can be easily integrated into zone-type compartment fire models and that can be used in "stand-alone" analyses.

Figure 1, adopted from References [1] and [2], is a sketch of example wall system designs under consideration. In general, two arbitrary-thickness gypsum wall panels are mounted one on either side of an array of vertical steel studs. In practice, each of the two panels shown can involve a single thickness of gypsum board or a sandwich-type multiple-thickness design of two or more well-contacted boards. Figure 1 illustrates two possible assembly designs. One of these is referred to as a 1x1-type assembly, since each of the two panels involves a single layer of gypsum board. The other is a 1x2 assembly, since one panel is a single layer of gypsum board and the other involves a two-layer construction. The studs, separated at regular intervals, form an unfilled air gap between the panels. As is the case in practical implementations of these kinds of wall systems, the spacing of the studs is several times the thickness of the air gap. Also, the studs are typically fabricated from relatively thin-gage steel (the studs used in the experimental study of [1] were 0.46 mm thick) and they are not effective as paths for conductive heat transfer between the panels.

Extensive thermocouple data on the thermal response of a Figure-1 1x2-type wall system to ASTM E119 [3] standard-fire furnace exposures were acquired and presented in Reference [1]. These data indicate that the temperature distribution in the gypsum panels, even relatively close to the steel studs, were substantially one-dimensional through the thickness of the panels. Consistent with this finding and with an experimentally-validated thermal response model presented in [2] (all gypsum panels used in [1] and [2] were of fire-rated material), it will be generally assumed here that: 1) relative to effects of conduction heat transfer, the steel studs simply act as thermally insulating spacers for the gypsum panels, and 2) radiation exchanges across the air gap, between the facing surfaces of the gypsum panels, can be well-predicted by an analysis involving radiative exchange between two infinite parallel planes, i.e., the steel studs do not have a significant effect on modifying the radiation exchange between the facing panel surfaces. In the analysis to be presented here, the time-dependent thermal response of the gypsum panels will be simulated by an idealized system involving two initially uniform-temperature vertical gypsum board panels, infinite in extent and separated by an air gap, where the system is always heated at the two bounding outer surfaces by spatially-uniform heat fluxes.

THE GEOMETRY OF THE MODEL WALL SYSTEM

Figure 2 defines the generic geometry of the two-panel wall system under consideration. As seen in the figure, x is the distance measured normal to the panels, from left to right. The left- and right-hand panels are designated as panels 1 and 2, respectively, and $x = x_1 = 0$ is taken as the left surface

of panel 1, the other three surfaces being located at $x = x_2$, x_3, and x_4, where $x_1 = 0 < x_2 < x_3 < x_4$. The thicknesses of panel 1, the air gap, and panel 2, designated as L_1, L_{GAP}, and L_2, respectively, are:

$$L_1 = x_2 - x_1 = x_2;\ L_{GAP} = x_3 - x_2;\ L_2 = x_4 - x_3 \tag{1}$$

The enclosed rooms or open spaces to the left and right of panels 1 and 2 are designated as spaces 1 and 2 respectively. The surface located at $x = x_i$ is designated as surface i.

HEAT TRANSFER TO THE PANEL SURFACES

Define $\dot{q}_i''$ as the flux of heat transfer to a panel at surface i.

Outside-Facing Surfaces 1 and 4; General Considerations

The two-panel wall system being considered can be used as a barrier that separates enclosed spaces of a multi-room facility, or as a barrier that separates an inside space and the outside environment. Either, or both outward-facing surfaces of the wall system, surfaces 1 or 4, can be exposed to a fire-generated environment or to an ambient environment. In general, $\dot{q}_i''$, i = 1 or 4, will be a function of $T_i = T(x = x_i, t)$, ε_i, the effective gray-body emissivity of surface i, and of the variables that describe the environment in the space to which surface i is exposed.

$$\dot{q}_i'' = F_i(T_i, \varepsilon_i; \text{variables of the environment to which surface i is exposed}),\ i = 1 \text{ or } 4 \tag{2}$$

When spaces 1 and/or 2 involve fire environments, the specification for F_1 and F_4 will depend on the method chosen to describe or simulate the fire environment there, e.g., a method consistent with a particular room fire model adopted. To use the thermal wall model in a fire model simulation, it will be necessary to provide explicit functional relationships for the F_i.

Outside-Facing Surfaces 1 and 4; Simulating Furnace Test Exposures

This work describes a thermal model for Figure 1-type wall systems and verifies it using experimental data from ASTM E119 standard fire exposures as presented in [1] and [2]. For the verification, it will be necessary to provide relationships for F_i, i = 1 and 4 of Eq. (2), when the environment in one of these spaces, say space 1, corresponds to that found in a wall-furnace enclosure during a standard fire exposure, and when the environment in the other space, space 2, corresponds to that found in the laboratory space containing the wall furnace.

Heat transfer to the furnace-fire-exposed surface. Consider the rate of heat transfer to the furnace-fire-exposed surfaces of construction elements undergoing ASTM E119-type standard tests, where average furnace gas temperatures are specified to follow the standard time-temperature curve, $T_{STD}(t)$, as specified, for example, by ASTM E119 [3] or ISO 834 [4]. It is well-accepted that F_1, corresponding to such furnace test exposures, can be simulated by (see, e.g., [5] or [6])

$$\dot{q}''_1 = F_1 = F_{FUR} = h_{FUR}(T_{STD} - T_1) + [\sigma/(1/\varepsilon_{FUR} + 1/\varepsilon_1 - 1)](T^4_{STD} - T^4_1) \tag{3}$$

where ε_{FUR} is a combined, effective, gray-body, surface emissivity of the furnace walls and fire gases, ε_1 is the effective gray-body emissivity of surface 1, and σ, the Stephan-Bolzmann constant, and h_{FUR}, the heat transfer coefficient for convective transfer to the furnace-exposed surface of the system being tested, are given by

$$h_{FUR} = 25 \text{ W/(m}^2\text{K)}; \quad \sigma = 5.7(10^{-8}) \text{ W/(m}^2\text{K}^4\text{)} \tag{4}$$

On the right side of Eq. (3), the first term provides a rough estimate of the convective component of the heat transfer. It is a result of the relatively vigorous forced convection flows which are characteristic of a furnace environment. The second term is the radiative component of the heat transfer. A precise estimate of the convective heat transfer is not required since, for furnace temperatures and $(T_{FUR} - T_i)$ temperature differences of interest, the radiation term is typically much larger than convection term.

Heat transfer to the laboratory-exposed surface. Heat transfer to the ambient-environment-exposed surfaces would also have convective and radiative components. The latter would be characterized by radiative exchanges between surface 4 and a black-body far field radiating at the ambient temperature T_{AMB}. Assuming a relatively quiescent laboratory environment, any convective heat transfer to surface 4 would be a result of natural convection.

An estimate for heat transfer to a vertical surface of height H at uniform temperature T_4 from a quiescent atmosphere at $T_{AMB} < T_4$ can be obtained with the use of the heat transfer coefficient [7]

$$h_{AMB} = 1.3(T_4 - T_{AMB})^{1/3} \text{ W/(m}^2\text{K}^{4/3}\text{)} \tag{5}$$

for a turbulent boundary layer flow, provided

$$T_4 - T_{AMB} > 50 \text{ K/(H/m)}^3 \tag{6}$$

Eq. (5) will be used below. At times when Eq. (6) is not satisfied, it will be assumed that both actual and (poorly) estimated convective heat transfer at surface 4 would have a negligible effect on the overall thermal response of the wall system.

In view of the above, under standard fire test conditions F_4 will be taken to be

$$\dot{q}''_4 = F_4 = - h_{AMB}(T_4 - T_{AMB}) - \varepsilon_4 \sigma(T_4^4 - T_{AMB}^4) \tag{7}$$

Inside-Facing Surfaces 2 and 3; Simulating Heat Transfer Across the Air Gap

As differences between T_2 and T_3 begin to develop during the course of a fire exposure, $\dot{q}''_2$ and $\dot{q}''_3$ will have a radiative component, $\dot{q}''_{2,RAD}$ and $\dot{q}''_{3,RAD}$, occurring as a result of radiation exchanges through the air layer, and a component, $\dot{q}''_{2,CON}$ and $\dot{q}''_{3,CON}$, resulting from surface-to-air conduction/convection exchanges.

$$\dot{q}''_2 = \dot{q}''_{2,RAD} + \dot{q}''_{2,CON};\ \dot{q}''_3 = \dot{q}''_{3,RAD} + \dot{q}''_{3,CON} \tag{8}$$

For the purpose of calculating the radiation exchanges it is assumed that the air layer is transparent. Therefore [8]

$$\dot{q}''_{2,RAD} = [\sigma/(1/\varepsilon_2 + 1/\varepsilon_3 - 1)](T_3^4 - T_2^4) = - \dot{q}''_{3,RAD} \tag{9}$$

Assume that the heat capacity of the mass of air in the gap is negligible in the sense that a relatively small rate of energy transfer is required to maintain the average air temperature, T_{AIR}, at

$$T_{AIR} = (T_1 + T_2)/2 \tag{10}$$

Then, in terms of an effective thermal conductivity, k_{EFF}, the conduction/convection components can be estimated by the simple cross-gap-type conduction model [8]

$$\dot{q}''_{2,CON} = (k_{EFF}/L_{GAP})(T_3 - T_2) = - \dot{q}''_{3,CON} \tag{11}$$

where

$$k_{EFF}/k_{AIR} = f(GrPr);\ Gr = g(T_3 - T_2)L_{GAP}^3/(T_{AIR}\nu^2);\ Pr \approx 0.7 \tag{12}$$

In Eq. (12), Gr is a Grashoff number based on the air properties and the air gap thickness, g is the acceleration of gravity, and Pr and ν are the Prandtl number and kinematic viscosity, respectively, of air at temperature T_{AIR}. f(GrPr), from a correlation of experimental data [9], is plotted in Figure 11-14 of [8]. A curve fit for these data is [10]

$$f(GrPr) = \begin{cases} 1, & \log(GrPr) < 3; \\ 0.11(GrPr)^{0.29}, & 3.8 < \log(GrPr) < 6; \\ 0.40(GrPr)^{0.20}, & 6 < \log(GrPr) < 8 \end{cases} \tag{13}$$

f(GrPr) of Eq. (12) is such that f is monotonically increasing with GrPr, approaching 15.8 at GrPr = 10^8. For problems of interest here, GrPr will likely never exceed 10^7, corresponding to f = 10, and k_{AIR} would fall in the range, 0.035 W/(mK) < k_{AIR} < 0.070W/(mK) . For example, using Eqs. (10)-(13) consider test data presented in Figure 11 of [1] (L_{GAP} = 0.09 m) at the relatively early and late times, 10 and 30 min, respectively:

at t = 10 min: T_2 = 380 K; T_3 = 355 K:

T_{AIR} = 368 K; k_{AIR}= 0.031 W/(mK); ν_{AIR}= 3.2(10^{-5}) m^2/s;

GrPr = 3.3(10^5); f = k_{EFF}/k_{AIR} = 4.4; $\dot{q}''_{2,CON}$ = 38 W/m^2; $\dot{q}''_{2,RAD}$ = 280 W/m^2

(14)

at t = 30 min: T_2 = 790 K; T_3 = 690 K:

T_{AIR} = 740 K; k_{AIR} = 0.054 W/(mK); ν_{AIR}= 7.2(10^{-5}) m^2/s;

GrPr = 1.3(10^5), f = k_{EFF}/k_{AIR} = 3.3; $\dot{q}''_{2,CON}$ = 198 W/m^2; $\dot{q}''_{2,RAD}$ = 9300 W/m^2

The above estimates suggest that for the type of problem considered here (i.e., for wall heating problems where temperature increases of the gypsum panels are considered to be significant when they are of the order of several hundred K), when the net rate of heat transfer across the gap starts

to become significant, $\dot{q}''_{2,RAD} >> \dot{q}''_{2,CON}$. Based on this it is convenient to use the approximation:

$$\dot{q}''_2 = - \dot{q}''_3 = \dot{q}''_{2,RAD} \tag{15}$$

A MODEL FOR THE THERMAL RESPONSE OF THE GYPSUM PANELS

Heating of the Gypsum

At ambient temperature and prior to any heating, gypsum panels are made up of calcium sulfate dihydrate, $CaSO_4 \cdot 2H_2O$, that contains about 21% by weight of chemically-combined water, and additional, relatively-small amounts of absorbed free water [11]. Also, practical Figure 1-type wall systems include a relatively-thin paper covering on the exposed surfaces of the gypsum panels. In the fire tests of [1], this paper, approximately 0.4 mm thick, was observed to burn off within 3 min of the start of the test. The analysis for the thermal response of the gypsum panels, to be developed here, will ignore the effects of such surface-mounted paper.

When the temperature of a panel is raised above 80 °C, the chemically-bound water begins to be released in a process that involves two stages. Most of the water is released in the first stage, as the $CaSO_4 \cdot 2H_2O$ becomes calcium sulfate hemihydrate, $CaSO_4 \cdot 1/2H_2O$ (plaster of Paris). This stage is usually complete by the time the material reaches 125 °C. As heating is continued, the rest of the water is released and the remaining material goes to anyhydrous calcium sulphate, $CaSO_4$. During these processes, when the material is at and above the boiling temperature, absorbed and released water goes to the gaseous phase in a process that requires the absorption of relatively large amounts of energy. The reader is referred to Reference [11] for more detail of these processes, and for further reference to other relevant literature.

When the steam is released in depth, moisture migration must occur before it can actually reach one or the other bounding surfaces and be released to the adjacent atmosphere. Also, the migration of moisture toward the relatively-cool in-depth portion of the gypsum can lead to recondensation of the water vapor, which will, in turn, lead to some modification locally to the permeability of the gypsum. Some details of modeling the moisture migration are presented in Reference [12].

Modeling the Thermal Response of the Gypsum and Its Thermal Properties

Both gypsum panels of a particular wall system design are assumed to have identical properties.

A conduction heat transfer analysis of the thermal response of Figure 1-type wall systems to ASTM E119-type furnace heating is presented in [2]. The analysis uses a temperature-dependent, specific-heat model for the gypsum panels that is deduced directly from differential scanning calorimeter measurements, at 2°C/min, on a relatively-small 40 mg sample. Note that representation of specific heat in the conduction equation based on such small-sample data is equivalent to an assumption that

1) the thickness of the panels are small enough for substantially unrestricted moisture migration to occur and 2) any effects of recondensing water vapor are not significant.

As reported in [2], and especially at times when T_2 and T_3 exceed approximately 200 °C, wall model simulations of ASTM E119-type fire resistance tests were shown to compare favorably with experimental data. Experimental data presented in [2] include the above-mentioned test data of [1]. All these data were acquired with gypsum panels and gypsum samples of fire-rated Type X material.

Reference [11] develops a two-dimensional heat conduction model for a Figure 1-type wall system (same thickness panels as in [2]), where wood studs replace steel studs and where the thermal response of the wood studs is an important and desired feature of that analysis. In the part of the model that deals with the response of the gypsum panels, it is assumed, in contrast to [2], that significant moisture migration does not occur. In particular, subsequent to the phase change of released water from liquid to steam, $C_p(T)$ is determined from an analysis that treats the gypsum as a combined solid/steam system. Finally, in [11], $\rho(T)$ is determined from thermogravimetric analyzer data acquired at a scanning rate of 20 °C/min and $k(T)$ from steady-state measurements.

As reported in [13], and, again, especially at times when T_2 and T_3 exceed approximately 200 °C, simulation results using an advanced version of the Reference-[11] model were shown to compare favorably with experimental data from ASTM E119-type fire resistance tests.

Wall models like those of [2], [11], and [13] that depend on a straight-forward conduction equation analysis and use of effective, temperature-dependent thermal properties can only be expected to yield accurate results to the extent that details of moisture migration phenomena, including the details of local moisture-dependent property variations are not significant. The favorable results mentioned above of the models of [2], [11], and [13], suggest that when the gypsum exceeds approximately 200 °C, moisture-dependence of the properties and moisture migration details can be so ignored.

The reader is referred to References [14], [15], and [16] for additional insight on modeling the thermal response of the gypsum and its thermal properties.

Representations for the Density, Specific Heat, and Thermal Conductivity of Gypsum

In modeling the thermal response of Figure-1-type wall systems to fire exposures, especially in applications of present interest where simulations to temperatures of 200 °C and higher are of particular interest, it will be assumed here, consisent with the above discussion, that: 1) the thermal response of the gypsum panels can be deduced from a traditional heat conduction model that uses $\rho(T)$, $C_p(T)$, and $k(T)$ representations determined with the use of traditional property-measurement techniques, and 2) the details of moisture migration can be ignored.

The wall model to be developed here will be verified with the wall furnace test data of [1] and [2]. $\rho(T)$, $C_p(T)$, and $k(T)$ of the gypsum panels used in those tests were measured under quasi-steady-state temperature conditions and reported in [2] as linear interpolations between [property,

temperature] data pairs.

Property representations used here for wall-model validation and presented in **APPENDIX A** are based on the property representations of [2]. The $\rho(T)/\rho(T = 20\ ^{\circ}C)$, $C_p(T)$, and $k(T)$ representations are plotted in Figures 3 - 5, respectively.

THE INITIAL/BOUNDARY-VALUE PROBLEM FOR THE THERMAL RESPONSE OF THE WALL SYSTEM

The objective of this work is an algorithm for determining the temperature distribution $T(x, t)$ in the gypsum wall panels of a Figure-2-type wall system for any time t, $t_1 < t \leq t_2$, for specified initial condition, $T_{INIT}(x) = T(x, t_1)$. The algorithm must solve the following generic initial/boundary-value problem:

Find $T(x, t)$ for $t_1 < t \leq t_2$ and $x_1 \leq x \leq x_2$ or $x_2 < x_3 \leq x \leq x_4$ satisfying

$$\rho(T)C_p(T)\partial T/\partial t = k(T)\partial^2 T/\partial x^2 + (\partial k/\partial x)(\partial T/\partial x) \tag{16}$$

subject to the initial conditions:

$$T(x, t = t_1) = T_{INIT}(x) \tag{17}$$

for specified $T_{INIT}(x)$, and the boundary condition:

$$\text{at } x = x_1\text{: } T = T_1(t) \text{ or } k(T)\partial T/\partial x = -\dot{q}''_1(t) \tag{18}$$

$$k(T)\partial T/\partial x \Big|_{x = x_2} = k(T)\partial T/\partial x \Big|_{x = x_3} = [\sigma/(1/\varepsilon_2 + 1/\varepsilon_3 - 1)][T(x_3, t)^4 - T(x_2, t)^4] \tag{19}$$

$$\text{at } x = x_4\text{: } T = T_4(t) \text{ or } k(T)\partial T/\partial x = \dot{q}''_4(t) \tag{20}$$

for specified $T_1(t)$ or $\dot{q}''_1(t)$ and $T_4(t)$ or $\dot{q}''_4(t)$.

In the above, note that Eq. (19) follows from Eqs. (9) and (15).

When the specific problem of interest is to find the response of the wall system to a standard fire furnace exposure, the problem involves the following explicit conditions:

When surface 1 is exposed to a standard fire furnace exposure, the initial condition of Eq.

(17) becomes

$$T(x, t = 0) = T_{AMB} = T_{STD}(t = 0) \tag{17'}$$

for specified T_{AMB}, and the boundary conditions of Eqs. (18) and (20) become

$$\text{at } x = x_1\text{: } k(T)\partial T/\partial x = - h_{FUR}(T_{STD} - T) - [\sigma/(1/\varepsilon_{FUR} + 1/\varepsilon_1 - 1)](T^4_{STD} - T^4) \tag{18'}$$

$$\text{at } x = x_4\text{: } k(T)\partial T/\partial x = - h_{AMB}(T - T_{AMB}) - \varepsilon_4\sigma(T^4 - T^4_{AMB}) \tag{20'}$$

where recommended values for h_{FUR} and h_{AMB} are given in Eqs. (4) and (5), respectively.

THE INITIAL/BOUNDARY VALUE PROBLEM IN TRANSFORMED VARIABLES

The algorithm for solving Eqs. (16)-(20) will use a computer software solver that motivates redefinition of the problem in terms of the following transformed spatial variables and new dependent and independent variables:

For $x_1 \le x \le x_2$:

$$\begin{aligned} &T^{(1)} = T;\ \partial T^{(1)}/\partial X = \partial T/\partial x;\ X = x - x_1 \text{ (i.e., } 0 \le X \le L_1); \\ &\lambda_1 = \lambda_1(T^{(1)}) = 1/[\rho(T^{(1)})C_p(T^{(1)})];\ \kappa_1 = \kappa_1(T^{(1)}) = k(T^{(1)})\lambda_1(T^{(1)}) \end{aligned} \tag{21}$$

For $x_3 \le x \le x_4$:

$$\begin{aligned} &T^{(2)} = T,\ \partial T^{(2)}/\partial X = - (L_1/L_2)\partial T/\partial x;\ X = L_1[1 - (x - x_3)/L_2] \text{ (i.e., } 0 \le X \le L_1); \\ &\lambda_2 = \lambda_2(T^{(2)}) = (L_1/L_2)^2/[\rho(T^{(2)})C_p(T^{(2)})];\ \kappa_2 = \kappa_2(T^{(2)}) = k(T^{(2)})\lambda_2(T^{(2)}) \end{aligned} \tag{22}$$

In the transformed variables of Eq. (22): the original depth of panel 2, L_2, is expanded/contracted to L_1, the depth of panel 1; the laboratory-exposed surface of panel 2, originally at its right side, is transformed to its left side, at the new origin, $X = 0$; and the cavity-exposed surface of panel 2, originally on the left, is transformed to the right side, at $X = L_1$. The transformation of Eq. (22) is depicted in Figure 2.

Then the problem of Eqs (16) - (20) becomes:

Find $T^{(1)}(X, t)$ and $T^{(2)}(X,t)$ for $t_1 < t \leq t_2$ and $0 \leq X \leq L_1$ satisfying

$$\partial T^{(1)}/\partial t = \kappa_1(T^{(1)})\partial^2 T^{(1)}/\partial X^2 + \lambda_1(T^{(1)})(\partial k/\partial X)(\partial T^{(1)}/\partial X)$$
$$\partial T^{(2)}/\partial t = \kappa_2(T^{(2)})\partial^2 T^{(2)}/\partial X^2 + \lambda_2(T^{(2)})(\partial k/\partial X)(\partial T^{(2)}/\partial X) \quad (23)$$

subject to the initial conditions

$$T^{(1)}(X, t = t_1) = T_{INIT}(x = X + x_1); \; T^{(2)}(X, t = t_1) = T_{INIT}(x = x_3 + L_2 - XL_2/L_1, t_1) \quad (24)$$

and the boundary conditions

at $X = 0$:

$$T^{(1)} = T_1(t) \text{ or } k(T^{(1)})\partial T^{(1)}/\partial X = - \dot{q}''_1(t); \quad (25)$$

$$T^{(2)} = T_4(t) \text{ or } k(T^{(2)})\partial T^{(2)}/\partial X = - \dot{q}''_4(t) \quad (26)$$

at $X = L_1$:

$$k(T^{(1)})\partial T^{(1)}/\partial X = - (L_2/L_1)k(T^{(2)})\partial T^{(2)}/\partial X = [\sigma/(1/\varepsilon_2 + 1/\varepsilon_3 - 1)](T^{(1)4} - T^{(2)4}) \quad (27)$$

When surface 1 is exposed to a standard fire furnace exposure, the initial conditions of Eq. (24) become

$$T^{(1)}(X, \; t = 0) = T^{(2)}(X, \; t = 0) = T_{AMB} \quad (24')$$

and the boundary conditions, Eqs (25) and (26), become

at $X = 0$:

$$k(T^{(1)})\partial T^{(1)}/\partial X = - h_{FUR}(T_{STD} - T^{(1)}) - [\sigma/(1/\varepsilon_{FUR} + 1/\varepsilon_1 - 1)](T^4_{STD} - T^{(1)4}) \quad (25')$$

$$k(T^{(2)})\partial T^{(2)}/\partial X = h_{AMB}(T^{(2)} - T_{AMB}) + \varepsilon_4 \, \sigma(T^{(2)4} - T^4_{AMB}) \quad (26')$$

SOLVING THE PROBLEM

The Subroutine *GYPST*

The FORTRAN 77 subroutine ***GYPST*** and associated computer software was developed to solve the initial/boundary-value problem of Eqs. (16) - (20). The subroutine uses the software ***MOLID*** [17], which solves for $T^{(1)}(X, t)$ and $T^{(2)}(X, t)$ of the transformed problem of Eqs. (23) - (27). Once these have been obtained, then, following Eqs. (21) and (22), the T(x, t) solution of the original problem is retrieved according to:

For $0 \le X \le L_1$:

$$T = T^{(1)},\ \partial T/\partial x = \partial T^{(1)}/\partial X,\ x = x_1 + X\ ,\ \text{i.e.,}\ x_1 \le x \le x_2$$

$$T = T^{(2)},\ \partial T/\partial x - (L_2/L_1)\partial T^{(2)}/\partial X,\ x = x_3 + L_2 - X\,L_2/L_1\ \text{i.e.,}\ x_3 \le x \le x_4 \qquad (28)$$

Solving the Transformed Problem with *MOLID*

The transformed problem of Eqs. (23) - (27) is solved with ***MOLID*** [17]. This is a set of FORTRAN subroutines that provides for the method-of-lines solution for systems of initial-boundary-value partial differential equations in one space dimension, including systems that involve linear and non-linear parabolic equations subject to a wide variety of boundary conditions.

In ***MOLID***, spatial derivatives are approximated using either 2nd, 3rd, or 6th-order accurate finite differences on an equi-spaced grid. (In the present use of ***MOLID***, 2nd-order accurate finite differences are used.) The resulting ordinary initial value problem is then solved using the adaptive integration routine of [18]. In the calculation, estimates of the time step error at the spacial grid points are kept less than a user-specified, time-integrator, local-error, tolerance parameter EPSCAL. (In most example calculations to be presented below, EPSCAL is specified to be 0.00001.)

Using *GYPST*

To solve a particular wall-system fire-exposure problem with ***GYPST***, one must first specify T(x, t = TINT) at each of NPTS equi-distant nodes in panel 1 and NPTS equi-distant nodes in panel 2. Then, a call to the subroutine ***GYPST*** with this and other input data leads to a calculation of the thermal response of the wall system, subjected to one of nine possible sets of boundary conditions, between t = TINT and specified time t = TLAST. The set of boundary conditions of interest is identified by the input value IBCTYP = 1 - 9. The ***GYPST*** output yields the newly calculated T(x, t = TLAST) at each of the 2NPTS node points of the two panels. If the specified IBCTYP set of boundary conditions is one that does not explicitly specify heat transfer rates at surfaces 1 and 4, then the ***GYPST*** output also yields newly calculated values of these heat transfer rates.

The choices of boundary conditions include IBCTYP = 5, which is used in all ***GYPST*** simulations to be discussed below. This corresponds a simulation of the scenario where a specified wall system is subjected to an ASTM E119 fire furnace test. In particular, all ***GYPST*** simulations to be presented below will involve use of Eqs. (17') and (18') with T_{STD} calculated according to [2]

$$T_{STD}(t) = T_{ASTM\ E119}(t) \tag{29}$$

$$= T_{AMB} + 750.\{1.- \exp[- 3.79553(t/3600)^{1/2}]\} + 170.41(t/3600)^{1/2};\ t \text{ in [s]},\ T\text{'s in } ^{\circ}C$$

A concise description of ***GYPST***, extracted from the ***GYPST*** source code, is presented in **APPENDIX B**. This includes brief explanations of all options for boundary conditions and definitions of all parameters of the subroutine call sequence.

SIMULATING FURNACE EXPOSURE TESTS OF REFERENCES [1] AND [2]; VERIFICATION OF THE WALL MODEL

Standard Fire Furnace Tests on Two Different Figure-1-Type Wall Systems

Extensive tabulated thermocouple data on the thermal response of a full-scale, 3.0 m (width) x 3.7 m (height), Figure-1-type wall system to standard-fire furnace exposures were acquired and presented in Reference [1] (refer to the test of Assembly F-07). The wall system tested was a 1x2-type assembly, where the single-layer panel was the one exposed to the furnace environment. In the particular case of the F-07 wall design, all panels were 0.0127 m thick, i.e., a 0.0127 m thick gypsum panel on the fire-exposed side of the studs and a 0.0254 m-thick two-panel-sandwich arrangement on the other. Assembly F-07 test data are also presented in Figure 9 of [2]. This assembly and test will be referred to below as the "1x2 assembly/test."

In the 1x2 test, the furnace was operated to reproduce the CAN/ULC-S101-M89 [17], standard-fire temperature-time curve, which is similar to ASTM E119 [2].

In Figure 8 of Reference [2] there are also presented plotted test data of the thermal response of another 3.0 m x 3.7 m Figure-1-type wall system, which was also subjected to an ASTM E119-type exposure. This assembly was a 1x1-type design, where the panels used were each 0.0159 m thick. This will be referred to below as the "1x1 assembly/test."

Location of Temperature Measurements

During the tests, temperatures of the assemblies were measured by thermocouples that were attached to gypsum panel and steel stud surfaces at different elevations and at different lateral positions of the assembly. Of interest here are the temperatures on the gypsum panel surfaces. Generic locations

of relevant thermocouples, indicated in Figure 1, were:

- Fire-exposed panel:

  surface exposed to the cavity; (as in [2] refer to these as) **BL/Cav.[exp.]**

  Unexposed panel(s):

  surface exposed to the cavity; **BL/Cav.[unexp.]**

  contact surface between the two panels (only for 1x2 assembly); **BL/FL[unexp.]**

  surface exposed to the ambient/laboratory, where the thermocouples were unprotected; **UnExp.[bare]**

  surface exposed to the ambient/laboratory, where the thermocouples were protected by insulating pads; **UnExp.[under pads]**. (Since these thermocouples are protected from radiative heat transfer exchanges, they presumedly yield measurements of the temperatures of the surfaces to which they are attached that are more accurate than those of the **UnExp.[bare]** thermocouples.)

The reader is referred to References [1] and [2] for details of thermocouple locations.

Unless stated otherwise, in the case of the 1x2 test, experimental data plotted below for temperatures at the above generic locations will always refer to average temperatures as reported in Table 3 of [1] and as plotted in Figure 9 of [2]. Note that the data for **BL/FL[unexp.]**, which is from Table 3 of [1], does not appear in Figure 9 of [2]. When data from individual thermocouples at the **BL/Cav.[exp.]** locations (thermocouples 28, 29, 32, 33, 36, and 37) and the **BL/Cav.[unexp.]** locations (thermocouples 30, 31, 34, 35, 38, and 39) are plotted (e.g., in Figure 9), these are taken from Table 2 of [1].

In the case of the 1x1 test, experimental data to be presented below will always refer to average temperatures as plotted in Figure 8 of [2].

From the above referenced data, T_{AMB} for the 1x2 and 1x1 test are taken to be 26 °C and 23 °C, respectively.

Simulating the 1x1 and 1x2 Tests With *GYPST*

In addition to the already-specified parameters of the 1x1 and 1x2 tests, ***GYPST*** will require inputs for ε_i, i = 1 - 3, ε_{FUR}, and NPTS. The effect of varying these parameters will be studied in the various simulations to be reported below. All specified parameters of the 1x2 and 1x1

assemblies/tests and their ***GYPST*** simulations are summarized in Table 1.

Note in Table 1 that in the 1x2 assembly/test simulations, odd numbers, 11 and 21, were chosen for NPTS. This was done for convenience, so that for the unexposed panel, panel 2, the location of the middle node point would correspond exactly to the location of the contact surface, between its two "sandwiched" gypsum panels, where the **BL/FL[unexp.]** thermocouple data were acquired.

Other Details of the Simulations

For every simulation to be presented, the simulation test time was set at 4200 s. The wall-system reponse for the entire duration of the test was determined from 140 separate 30 s calls to ***GYPST*** (i.e., TLAST = TINT + 30.), where the temperature output at the model node points from one 30 s simulation interval was used as the temperature input at these same node points for the next 30 s interval. All calculations were carried out on a PC with a 90 MHz Pentium processor.

Expected Limits for the *GYPST* Simulations

For both the 1x2 and 1x1 assemblies/tests, the measured temperatures of the two cavity-exposed surfaces, surfaces 2 and 3 became nearly equal, in an abrupt manner, as they reached approximately 600 °C. This was interpreted in [2] as indication of a failure in panel 1, and led to the conclusion that, for the two tests reported, the "gypsum board is no longer in place when [throughout its thickness] its temperature exceeds 600 °C." Since the wall model can not be expected to provide valid simulations when one of the panels is "no longer in place," e.g., when a portion of the fire-exposed panel cracks and falls away, the validity of the present ***GYPST*** simulations cannot be expected to go beyond the time when the temperature of surface 2, **BL/Cav.[exp.]**, reaches 600 °C.

RESULTS OF *GYPST* SIMULATIONS OF THE 1X1 ASSEMBLY/TEST

This section presents results of ***GYPST*** simulations of the 1x1 assembly test.

GYPST Simulations Using Different Values of Emissivity

No guidance is available on the most appropriate values for characterizing the ϵ_i's for the gypsum surfaces. Similarly unavailable is the effective ϵ_{FUR} value for the particular furnace used to carry out the tests. Therefore, ***GYPST*** simulations of the test included a parameteric study involving several different sets of values for these emissivities. Two series (two different values of NPTS) of four ***GYPST*** simulations each (different values of ϵ_{FUR} and ϵ_i's) were carried out. In three of the four latter simulations, ϵ_{FUR} and all ϵ_i's were assumed to be identical, 0.9, 0.8, or 0.7. In the fourth simulation, all ϵ_i's were assumed to be 0.5 and ϵ_{FUR} was assumed to be 0.8 (since an assumed value of $\epsilon_{FUR} = 0.5$ is considered to be unreasonably low). The two series involved different levels of calculation-grid refinement, NPTS = 10 or 20. A third series considered the effect of changing the specified numerical precision parameter, EPSCAL.

Simulations with NPTS = 20: Results of ***GYPST*** temperature simulations with NPTS = 20 and the different values of emissivity are plotted with measured temperatures in Figures 6a-d. Included in the plots are: the calculated temperatures for the furnace-exposed surface of panel 1, designated as **Exp.**; the temperature of the furnace, T_{STD}, as determined from Eq. (29); and the temperatures calculated at locations corresponding to the locations **BL/Cav.[exp.]**, **BL/Cav.[unexp.]**, and **UnExp.[under pads]** (or **UnExp.[bare]**).

As can be seen in Figures 6a-c, when the ϵ_{FUR} and the ϵ_i's are 0.9, 0.8, or 0.7, the comparisons between simulated and measured temperature are very favorable (up to the time when the calculation is invalidated because of panel 1 failure, when the measured temperature at **BL/Cav.[exp.]** reaches approximately 600 °C), with comparisons improving with increasing emissivity. Of the three simulations, the two corresponding to $\epsilon_{FUR} = \epsilon_i = 0.9$ and 0.8 (Figures 6a and 6b) lead to the best comparisons between measured and calculated values, with little variation between the results in these two cases. In general, the dependence of simulated temperatures on emissivity is seen to be relatively weak in this 0.9 - 0.7 range of emissivity. However, a clear degradation in the comparison between measured and calculated temperatures is seen for the simulation of Figure 6d, where the ϵ_i's have been reduced to 0.5.

Calculation times for all the above simulations were approximately 160 s.

Reducing the value of NPTS and EPSCAL

If ***GYPST*** is to be used in zone-type fire model simulations, then computational time becomes a critical issue. For this reason it was of interest to explore the effect of reduction in NPTS and EPSCAL on simulation performance, in general, and on computational time, in particular.

Simulations with NPTS = 10: The previous simulations were carried out again with all parameters, except for NPTS, identical to those used previously. For this case NPTS was reduced to 10.

Calculation times for all the new simulations were reduced from approximately 160 s to approximately 25 s. The results of the particular simulation that corresponds to that of Figure 6a are presented in Figure 7. As can be seen from these two figures, the calculated temperatures for the new NPTS = 10 calculations do not compare as favorably to measured values as do the NPTS = 20 calculation results. Also, use of the relatively-coarse NPTS = 10 grid introduces "wiggles" into the calculated temperature histories. Nevertheless, at a significant savings in computational time, the new calculation provides results which still compare relatively well with the measured temperatures.

In the case of the Figure 6b-d-type simulations, the comparison of the NPTS = 10 to the NPTS = 20 results were similar to the Figure 6a/Figure 7 result.

Effect of increasing EPSCAL: Figure 6a-type simulations were carried out with all parameters, except for EPSCAL, identical to those used in the original simulation. EPSCAL was increased from 0.00001 to 0.0001, and then to 0.001, and .01. The calculation times for these three new simulations

remained in the range 160-155 s.

Results for the EPSCAL = 0.01 case are plotted in Figure 8. As can be seen, except for the predicted temperatures **Exp.** of the furnace-exposed surface of panel 1,where scatter of computed temperatures within a relativly narrow range can be observed, the difference between these results and those of Figure 6a, for EPSCAL = 0.00001, can not be detected visually.

When EPSCAL was increased to 0.1, after several of the 30 s-interval time steps, the calculation resulted in an "overflow," and the 4200 s simulation was not completed successfully.

RESULTS OF *GYPST* SIMULATIONS OF THE 1X2 ASSEMBLY/TEST

This section presents results of ***GYPST*** simulations of the 1x2 assembly test.

GYPST Simulations Using Different Values of Emissivity

Simulations were carried out for the 1x2 assembly/test with the same sets of ϵ's as for the 1x1 assembly/test, and with two different values of NPTS. Here, NPTS was chosen to be 11 or 21.

Simulations with NPTS = 21: Results of ***GYPST*** simulations with NPTS = 21 and the different values of emissivity (corresponding to those of Figures 6a-d) are plotted with measured temperatures in Figures 9a-d. Included in the plots are: the calculated temperatures for the furnace-exposed surface of panel 1, designated as **Exp.**; the temperature of the furnace, $\mathbf{T_{STD}}$, as determined from Eq. (29); and the temperatures calculated at locations corresponding to the locations **BL/Cav.[exp.]**, **BL/Cav.[unexp.]**, **BL/FL[unexp.]**, and **UnExp.[under pads]** (or **UnExp.[bare]**).

As can be seen in Figures 9a-c, and as was the case with the 1x1 asembly/test simulations of Figures 6a-c, when the ϵ_{FUR} and the ϵ_i's are 0.9, 0.8, or 0.7, the comparisons between simulated and measured temperature are very favorable (up to the time when the calculation is invalidated because of panel-1 failure, when the measured temperature at **BL/Cav.[exp.]** reaches approximately 600 °C), with comparisons improving with increasing emissivity. Of the three simulations, the two corresponding to $\epsilon_{FUR} = \epsilon_i = 0.9$ and 0.8 (Figures 9a and 9b) led to the best comparisons between measured and calculated values, again with little variation between the results in these two cases. Also, in the 0.9 - 0.7 range of emissivity, the dependence of simulated temperatures on emissivity is again seen to be relatively weak, where, in contrast to this, a clear degradation in comparison between measurements and calculations occurs when the ϵ_i's are reduced to 0.5 (see Figure 9d).

In the 1x2 assembly/test, where data from individual thermocouples are available from [1], it is interesting to get a sense of the relative variation of the different thermocouple measurements that make up the previously-plotted averages of the measured temperatures. Toward this end, all measured temperatures at the generic locations **BL/Cav.[exp.]** and **BL/Cav.[unexp.]** are plotted in Figure 10 together with the Figure 9a calculated values. It is seen from this plot that, for the 1x2

assembly/test and throughout the test times of interest, the characteristic variations of measured temperatures at cavity surface 2 and at cavity surface 3 are the same as the characteristic difference between the spacially-averaged temperatures of these two surfaces. The plot also reveals clearly the development of the failure of panel 1 as the temperature throughout its depth uniformly exceeds approximately 600 °C.

Calculation times for all above 1x2 assembly/test simulations were approximately 270 s.

Simulations with NPTS = 11: Figure 6-type simulations were carried out with all parameters, except for NPTS, identical to those used previously. Here, NPTS was reduced to 11.

Calculation times for all the new simulations were reduced from approximately 270 s to 45 s. The results of the particular simulation that corresponds to that of Figure 9a are presented in Figure 11. As can be seen from Figures 9a and 11, and as was the case in the 1x1 assembly/test simulations the calculated temperatures for this new reduced-NPTS calculation do not compare as favorably to measured values as do the NPTS = 21 calculation results. Again, use of the relatively-coarse NPTS grid has introduced "wiggles," here even more pronounced then for the 1x1 test, into the calculated temperature histories. And again, at significant savings in computational time, the new calculation provides results which still compare relatively well with the measured temperatures.

In the case of the Figure 9b-d-type simulations, the comparison of the NPTS = 11 to the NPTS = 21 results were similar to the Figure 9a/Figure 11 result.

GYPST Simulations With "Nearly"-Discontinuous Density and Thermal Conductivity Representations

As discussed and as presented in APPENDIX A and in Figures 3-5, all the above ***GYPST*** simulations use gypsum properties where Reference-[2]-recommended, discontinuous, step changes of $\rho(T)$ and $k(T)$, at T = 80 °C and 100 °C, respectively, are represented by corresponding changes over a 20 °C interval.

It is of interest to study the effect on a ***GYPST*** simulation of using property representations that are "more-nearly" discontinuous, e.g., more in keeping with the Reference [2] recommendations, with significant changes in properties being represented as occuring over intervals of only a few °C. Toward this end, one additional calculation was carried out, identical to that of Figure 9a, except that temperature-dependent changes of $\rho(T)/\rho(T = 20\ °C)$ and $k(T)$, centered at T = 80 °C and 100 °C, respectively, and taking place over a 20 °C interval, are now represented as taking place over a 2 °C interval (i.e., 70 and 90 of Table A-2 are replaced by 79 and 81, respectively, and the 90 and 110 of Table A-4 are replaced by 99 and 101, respectively).

The result of the new simulation is presented in Figure 12, which is to be compared to Figure 9a. As can be seen, except for the calculated temperature at the thermocouple location **BL/Cav.[unexp.]** (i.e., at the cavity-exposed surface of panel 2), and then only when temperatures there are less than

400 °C, differences in the two results are hardly noticeable.

Compared to the calculation time of the Figure 9a simulation, calculation time for that of Figure 12 was unchanged at approximately 270 s.

The above comparisons indicate that, computationally, ***GYPST*** simulations are robust when dealing with "nearly"-discontinuous $\rho(T)$, $C_p(T)$, and $k(T)$ representations. However, they also indicate that some care in representing the real "smoothed" nature of the temperature dependence of these properties (i.e., significant property changes over several °C *vs* possibly unrealistic "nearly"-discontinuous step changes) leads to greater confidence in the uniform accuracy of a simulation.

SUMMARY AND CONCLUSIONS

This work developed a methodology and an associated FORTRAN subroutine, ***GYPST***, for solving an initial-value/boundary-value problem to simulate the thermal response of fire-environment-exposed wall systems constructed of two gypsum panels of arbitrary thickness mounted one on each side of an array of steel studs. ***GYPST*** calculates time-dependent temperatures through the thickness of the panels at equidistant sets of node points.

The wall model was verified by using ***GYPST***, in its stand-alone mode, to simulate the ASTM E119 furnace-fire test performance of two different wall system designs, where results of furnace tests on the two designs are reported in [1] and [2]. Calculated temperature response of the gypsum panel surfaces for both of the wall designs compared favorable with measured temperatures when ***GYPST***-user-specified panel-surface and furnace emissivities were specified in the range 0.7 - 0.9. Excellent results were achieved when all emissivities were chosen to be 0.8 or 0.9, with little variation in results between these two cases.

The ASTM E119 simulations showed that very favorable comparisons between calculation and experiment, obtained with 20 or 21 node points per panel (for the two wall design systems), were degraded, but were still useful, when the number of node points were reduced to 10 or 11. This halving of the number of node points reduced computation times to a sixth of their original values, from 270 s to 45 s for one of the wall design systems, and from 160 s to 25 s in the case of the other.

In ***GYPST***, temperature-dependent properties for the gypsum panels are determined by linear interpolation between user-supplied (property, temperature) data pairs. Data pairs used for all ***GYPST*** simulations discussed in this work were based on measured properties of the gypsum material used in the tested wall systems of [1] and [2].

The product of the above is an experimentally-verified, modular, thermal-wall-model algorithm and associated computer subroutine, ***GYPST***, that can be integrated into zone-type compartment fire models and that can also be used for a variety of "stand-alone" simulations, including simulations to determine the ASTM E119 furnace-fire test performance of some wall systems.

NOMENCLATURE

F_{FUR}	F_1 for furnace-exposed surface 1
F_i	function for determining $\dot{q}''_i$, Eq. (2)
f(GrPr)	Eq.(12)
Gr	Grashoff number, Eq. (12)
g	acceleration of gravity
H	height of the wall system
h_{AMB}	heat transfer coefficient, surface-to-ambient, Eq. (5)
h_{FUR}	heat transfer coefficient, surface-to-furnace, Eq. (4)
k_{EFF}	effective k of the air gap, Eq. (12)
L_1, L_2, L_{GAP}	Eq. (1)
Pr	Prandtl number of air
$\dot{q}''_i$	net rate of heat transfer to surface I
$\dot{q}''_{2,CON}$, $\dot{q}''_{3,CON}$	concective components of $\dot{q}''_2$, $\dot{q}''_3$
$\dot{q}''_{2,RAD}$, $\dot{q}''_{3,RAD}$	radiative components of $\dot{q}''_2$, $\dot{q}''_3$
T	temperature
T_{AMB}	ambient temperature
$T^{(1)}$, $T^{(2)}$	T in the right, left panel, see Figure (2).
T_{AIR}	characteristic T of the air in the gap, Eq. (10)
T_{INIT}	$T(x, t = t_1)$
T_i	T of surface i
T_{STD}	T(t) for a standard fire

t	time
X	transfromed x, Eq. (21)
x	distance, see Figure. (2)
x_i	x of surface i
ε_{FUR}	effective emissivity of furnace walls and gases
ε_i	emissivity of surface I
κ_1, κ_2	Eqs. (21), (22)
λ_1, λ_2	Eqs. (21), (22)
ν	kinematic viscosity of the air
σ	Stephan-Bolzmann constant, Eq. (4).

REFERENCES

[1] Sultan, M.A., *et al*, Temperature Measurements in Full-Scale Insulated and Non-Insulated (1x2) Gypsum Board Protected Wall Assemblies with Steel Studs; Internal Rpt. 675, National Research Council Canada (NR) Institute for Research in Construction, 1994.

[2] Sultan, M.A., A Model for Predicting Heat Transfer Through Non-Insulated Unloaded Steel Stud Gypsum Board Wall Assemblies Exposed to Fire, Fire Technology, Vol. 32, No. 3, pp.239-259, 1996.

[3] Standard Methods of Fire Tests of Building and Construction Materials, ASTM E119, ASTM Committee E-5, Subcommittee E05.11, American Society for Testing and Materials (ASTM), Philadelphia, August 1988.

[4] Fire Resistance Tests - Elements of Building Construction, ISO-834, International Organization for Standardization, Switzerland, 1992.

[5] Eurocode on Actions on Structures, Commission of the European Communities, Draft, p. 9, April 1990.

[6] Milke, J., Analytic Methods for Determining Fire Resistance of Steel Members, Section 3/Chapter 6, SFPE Handbook of Fire Protection Engineering, DiNenno, P.J. et al, Eds., 1st Edition, Society of Fire Protection Engineers, Boston, p. 3-100, 1988.

[7] Baumeister, T. And Marks, L.S., Eds., Standard Handbook for Mechanical Engineers, 7th Edition, McGraw Hill, p. 4-103, 1958.

[8] Eckert, E.R.G., and Drake, R.M., Heat and Mass Transfer, 2nd Edition, McGraw Hill, pp. 331-332, 1959.

[9] Kraussold, H., *et al*, Forschung a.d. Gebiete d. Ingenieurw, 5, pp. 186-191, 1934.

[10] Jacob, M., Heat Transfer, Vol. 1, John Wiley, p. 542, 1949.

[11] Mehaffey, J.R., Cuerrier, P., and Carisse, G., A Model for Predicting Heat Transfer Through Gypsum-Board/Wood-Stud Walls Exposed to Fire, Fire and Materials, 18, pp. 297-305, 1994.

[12] Hurst, J.P., and Ahmed, G.N., Modeling the Thermal Response of Gypsum Wallboard and Stud Assemblies Subject to Standard Fire Testing, Proceedings of the 1995 International Conference on Fire Research and Engineering, Orlando, D.P. Lund, Ed., Society for Fire Protection Engineers, Boston, pp. 568-573, 1995.

[13] Mehaffey, J.R. and Tekeda, H, Predicting Heat Transfer Through Wood-Stud Walls Exposed to Fire, Proceedings of the 1995 International Conference on Fire Research and Engineering, Orlando, D.P. Lund, Ed., Society for Fire Protection Engineers, Boston, pp. 557-562, 1995.

[14] Gerlich, J.T., Collier, P.C.R., and Buchanan, A.H., Design of Light Steel-framed Walls for Fire Resistance, Fire and Materials, 20, pp.79-96, 1996.

[15] Collier, P.C.R., A Model for Predicting the Fire-Resisting Performance of Small-Scale Cavity Walls in Realistic Fires, Fire Technology, pp. 120-136, 2nd Quarter, 1996.

[16] Thomas, G.C., Buchanan, A.H., Carr, A.J., Fleishmann, C.M., and Moss, P.J., Light Timber-Framed Walls Exposed to Compartment Fires, Jl. Fire Protection Engineering, 7(1), pp.25-35, 1995.

[17] Hyman, J.M., MOL1D, Rev. 1, Los Alamos Scientific Laboratory, Los Alamos, Oct. 1978.

[18] Hindmarsh, A.C., GEARB: Solution of Ordinary Differential Equations Having Banded Jacobian, University of California Report UCID-30059, March, 1975.

APPENDIX A: THE THERMAL PROPERTIES REPRESENTATIONS USED IN THE WALL MODEL

Linear Interpolation Between Specified Pairs of Property, Temperature Data Points

This Appendix presents the analytic representations used in the wall model for the properties $\rho(T)/\rho(T_{REF})$, $C_p(T)$, and $k(T)$ of the gypsum panels. All these are all defined by an algorithm, incorporated in the ***GYPST*** software, that involves linear interpolation in temperature between specified [property, temperature] data pairs and extrapolation at constant property beyond the extreme temperatures of these data pairs. For any particular property, the only requirement for a specified set of data pairs is that it be consistant with property values that are continous in temperature (i.e., step discontinuities are not allowed).

While particular gypsum board products can have a significant differences in ambient- temperature density, Reference [11] suggests that for any reference temperature, T_{REF}, the dimensionless density function $\rho(T)/\rho(T_{REF})$ is approximately invarient from one product to another. Based on this idea, the representation in ***GYPST*** for $\rho(T)$ of a particular product is obtained by the specified value $\rho(T = 20\ °C)$ of the product and by knowledge of the assumed-universal density function $\rho(T)/\rho(T = 20\ °C)$. Thus, if a representation of $\rho(T)/\rho(T = 20\ °C)$ is obtained from one set of measurements on one particular gypsum product, there is a basis for using it to estimate $\rho(T)/\rho(T = 20\ °C)$ for a wide range of other products.

Properties Representations Used in GYPST Simulations of the Tests of References [1] and [2]

Along with the measured value

$$\rho(20\ °C) = 698\ kg/m^3 \tag{A1}$$

the following data pairs are provided by Reference [2], to represent, *via* linear interpolation, measured values of $\rho(T)/\rho(T_{REF})$, $C_p(T)$, and $k(T)$ for the gypsum panels used in the tested wall systems of [1] and [2]:

<u>Density</u>:

$\rho(T)/\rho(T = 20\ °C)$	T [°C]
1.	70
0.825	90

(A-2)

Specific Heat:

C_p [J/(kgK)]	T [°C]
1500	20
1842	78
2769	85
5861	97
18479	124
2006	139
1001	148
714	373
715	430
571	571
618	609
3000	662
3070	670
571	685

(A-3)

Thermal Conductivity:

k [W/(m K)]	T [°C]
0.25	90
0.12	110
0.12	370
0.27	800
1.83	2000

(A-4)

Comment: Note that in Reference [1], $\rho(T)/\rho(T = 20\ °C)$ and $k(T)$ are represented as being discontinuous (i.e., step changes) at T = 80 °C and 100 °C, respectively. These approximations are represented here as changes that takes place continuously over 20 °C temperature intervals centered at 80 °C [see (A-2)] and 100 °C [see (A-4)], respectively. Other similar, but less obvious discontinuities also exist in the reference-[2] representation of $C_p(T)$ and $k(T)$. These discontinuities are removed in the present representations of these functions, i.e., linear interpolation between the data pairs of Eqs. (A-3) and (A-4).

Plots of $\rho(T)/\rho(T = 20\ °C)$, $C_p(T)$, and $k(T)$ from Eqs. (A-1)-(A-4) and the interpolation/extrapolation algorithm of ***GYPST*** are presented in Figures 3 - 5, respectively.

APPENDIX B: A DESCRIPTION OF THE GENERAL USAGE OF *GYPST* (FROM THE *GYPST* SOURCE CODE)

```
      SUBROUTINE GYPST(TEMP1,TEMP2,IXM,XM1,XM2,NPTS,IBCTYP,EPS1,EPS2,
     1      EPS3,EPS4,EPSFUR,EPSCAL,TINT,TLAST,TMP1IN,TMP4IN,TMP1FN
     2      ,TMP4FN,TAMB,Q1IN,Q1FN,Q4IN,Q4FN,AL1,AL2,ALGAP,DENAMB
     3      ,MRHOD,RHODDAT,MCP,CPDAT,MCOND,CONDDAT)
C*************************************************************************
C       THIS PROGRAM INTEGRATES THE INITIAL/BOUNDARY VALUE PROBLEM, BETWEEN TIME=TINT AND
C       TIME=TLAST, FOR THE TEMPERATURE OF A PAIR OF GYPSUM PANELS SEPARATED BY AN AIR GAP
C       AND HEATED ON EITHER EXPOSED SURFACE.  INPUT INCLUDES THE TEMPERATURE DISTRIBUTION
C       AT TIME=TINT AND AT NPTS EQUIDISTANT POINTS IN EACH OF THE TWO PANEL, INCLUDING A POINT
C       AT EACH PANEL SURFACE.  OUTPUT INCLUDES THE NEW TEMPERATURE DISTRIBUTION AT THE
C       SAME POINTS AND, IN THE CASE OF BOUNDARY CONDITIONS WHERE OUTER SURFACE HEAT
C       TRANSFER RATES ARE NOT EXPLICITLY SPECIFIED, THE NEW VALUES FOR THESE HEAT TRANSFER
C       RATES.
C
C       DEFINITIONS:
C
C       AL1
C               THICKNESS OF LEFT PANEL [M]
C       AL2
C               THICKNESS OF RIGHT PANEL [M]
C       ALGAP
C               THICKNESS OF AIR GAP [M]
C       CONDDATA(1,N)=CONDDAT(1,N), N=1,NCOND=MCOND
C               COND [W/(M*K)] OF NTH (COND,TEMP) DATA PAIR USED TO  CALCULATE  COND(TEMP)  IN
C               SUBROUTINE CONDGYP
C       CONDDATA(2,N)=CONDDAT(2,N), N=1,NCOND=MCOND
C               TEMP [C] OF  NTH  (COND,TEMP  DATA  PAIR  USED  TO  CALCULATE  COND(TEMP)  IN
C               SUBROUTINE CONDGYP
C       CPDATA(1,N)=CPDAT(1,N), N=1, NCP=MCP
C               CP [J/(KG*K)] OF NTH (CP,TEMP) DATA PAIR USED TO CALCULATE CP(TEMP) IN SUBROUTINE
C               DSPGYP
C       CPDATA(2,N)=CPDAT(2,N), N=1, NCP=MCP
C               TEMP [C] OF NTH (CP,TEMP) DATA PAIR USED TO CALCULATE CP(TEMP) IN SUBROUTINE
C               DSPGYP
C       DENAM
C               RHO OR DENSITY OF GYPSUM AT 20 C [KG/M**3]
C       EPS1,EPS2,EPS3,AND EPS4
C               THE EMISSIVITIES OF GYPSUM SURFACES 1, 2, 3, AND 4, RESPECTIVELY.
C       EPSFUR
C               EFFECTIVE EMISSIVITY OF THE FURNACE, FOR A STANDARD FIRE EXPOSURE OF SURFACE
C               1 OR OF SURFACES 1 AND 4, OR THE EFFECTIVE  EMISSIVITY  OF  THE  FIRE/FACING-
C               ROOM-SURFACES FOR ROOM FIRE EXPOSURES OF SURFACE 1 OR SURFACES 1 AND 4.
C       EPSCAL
C               THE SUBROUTINE USED TO CARRY OUT THE INTEGRATION IS MOL1D AND ITS ASSOCIATED
C               SUBROUTINES.  IN THIS, EPSCAL IS THE TIME INTEGRATOR LOCAL ERROR TOLERANCE.
C               PARAMETER ESTIMATES OF THE TIME STEP ERROR AT THE SPATIAL GRID POINTS FOR ALL
C               GRID POINTS FOR ALL THE PDES IS KEPT LESS THAN EPSCAL IN THE ROOT-MEAN-SQUARE
C               (RMS) NORM.  EPSCAL IS ALSO USED TO CHOOSE THE INITIAL STEP.
C       FIRE1DAT(1,N), N=1, NFIRE1
C               TEMPERATURE [K] OF NTH DATA PAIR (TEMPERATURE,TIME) USED IN SUBROUTINE FRTMP1
C               TO CALCULATE TMPFR1(TIME), THE TEMPERATURE VS TIME OF A FIRE ENVIRONMENT TO
C               WHICH SURFACE 1 IS EXPOSED WHEN IBCTYP = 7 OR 8; NFIRE1 =< 1000.
```

```
C     FIRE1DAT(2,N), N=1, NFIRE1
C           TIME [S] OF NTH DATA PAIR (TEMPERATURE,TIME) USED IN SUBROUTINE FRTMP1 TO
C           CALCULATE TMPFR1(TIME), THE TEMPERATURE VS TIME OF A FIRE ENVIRONMENT TO
C           WHICH SURFACE 1 IS EXPOSED WHEN IBCTYP = 7 OR 8; NFIRE1 =< 1000.
C     FIRE4DAT(1,N), N=1, NFIRE4
C           TEMPERATURE [K] OF NTH DATA PAIR (TEMPERATURE,TIME) USED IN SUBROUTINE FRTMP4
C           TO CALCULATE TMPFR4(TIME), THE TEMPERATURE VS TIME OF A FIRE ENVIRONMENT TO
C           WHICH SURFACE 4 IS EXPOSED WHEN IBCTYP = 8; NFIRE4 =< 1000.
C     FIRE4DAT(2,N), N=1, NFIRE4
C           TIME [S] OF NTH DATA PAIR (TEMPERATURE,TIME) USED IN SUBROUTINE FRTMP4 TO
C           CALCULATE TMPFR4(TIME), THE TEMPERATURE VS TIME OF A FIRE ENVIRONMENT TO
C           WHICH SURFACE 4 IS EXPOSED WHEN IBCTYP = 8; NFIRE4 =< 1000.
C     IBCTYP
C           TYPE OF BOUNDARY CONDITIONS:
C           IBCTYP = 1:   [Q1IN, Q1FN] AND [Q4IN, Q4FN] SPECIFIED; Q1 SPECIFIED AS A LINEAR
C                         INTERPOLATION IN TIME BETWEEN Q1IN, AT TIME TINT, AND Q1FN, AT TIME
C                         TLAST; Q4 SPECIFIED SIMILARLY BY Q4IN AND Q4FN.
C           IBCTYP = 2:   [Q1IN, Q1FN] AND [TMP4IN, TMP4FN] SPECIFIED; Q1 SPECIFIED AS LINEAR
C                         INTERPOLATION IN TIME BETWEEN Q1IN, AT TIME TINT, AND Q1FN, AT TIME
C                         TLAST; TEMPERATURE OF SURFACE 4 SPECIFIED SIMILARLY BETWEEN
C                         TMP4IN AND TMP4FN.
C           IBCTYP = 3:   [TMP1IN, TMP1FN] AND [Q4IN, Q4FN] SPECIFIED; TEMPERATURE OF
C                         SURFACE 4 SPECIFIED AS A LINEAR INTERPOLATION IN TIME BETWEEN
C                         TMP1IN, AT TIME TINT, AND TMP1FN, AT TIME TLAST; Q4 SPECIFIED
C                         SIMILARLY BY Q4IN AND Q4FN.
C           IBCTYP = 4:   [TMP1IN, TMP1FN] AND [TMP4IN, TMP4FN] SPECIFIED; TEMPERATURE OF
C                         SURFACE 1 SPECIFIED AS A LINEAR INTERPOLATION IN TIME BETWEEN
C                         TMP1IN, AT TIME TINT, AND TMP1FN, AT TIME TLAST; TEMPERATURE OF
C                         SURFACE 4 SPECIFIED SIMILARLY BETWEEN TMP4IN AND TMP4FN.
C           IBCTYP = 5:   Q1 SPECIFIED AS HEAT TRANSFER FROM AN ASTM E119 STANDARD-FIRE
C                         FURNACE ENVIRONMENT (TEMPERATURE-TIME ENVIRONMENT IS
C                         TMPSTD(TIME)) AND Q4 SPECIFIED AS HEAT TRANSFER FROM AN AMBIENT
C                         TEMPERATURE (TAMB) LABORATORY ENVIRONMENT.
C           IBCTYP = 6:   Q1 SPECIFIED AS HEAT TRANSFER FROM AN ISO 834 STANDARD-FIRE
C                         FURNACE ENVIRONMENT (TEMPERATURE-TIME ENVIRONMENT IS
C                         TMPSTI(TIME)) AND Q4 SPECIFIED AS HEAT TRANSFER FROM AN AMBIENT
C                         TEMPERATURE (TAMB) LABORATORY ENVIRONMENT.
C           IBCTYP = 7:   Q1 IS THE HEAT TRANSFER FROM A SPECIFIED ROOM-FIRE ENVIRONMENT
C                         (TEMPERATURE-TIME OF THE FIRE ENVIRONMENT IS TMPFR1(TIME), CAL-
C                         CULATED IN THE SUBROUTINE FRTMP1 BY INTERPOLATION/EXTRAPO-
C                         LATION OF DATA IN INPUT COMMON BLOCK FIRE1BLK) AND Q4 IS
C                         SPECIFIED AS HEAT TRANSFER FROM AN AMBIENT-TEMPERATURE (TAMB)
C                         LABORATORY ENVIRONMENT.
C           IBCTYP = 8:   Q1 IS THE HEAT TRANSFER FROM ONE SPECIFIED ROOM-FIRE
C                         ENVIRONMENT (TEMPERATURE-TIME OF THE FIRE ENVIRONMENT IS
C                         TMPFR1(TIME), CALCULATED IN THE SUBROUTINE FRTMP1 BY INTERPO-
C                         LATION/EXTRAPOLATION OF DATA IN INPUT COMMON BLOCK FIRE1BLK)
C                         AND Q4 THE HEAT TRANSFER FROM ANOTHER SPECIFIED ROOM-FIRE
C                         ENVIRONMENT (TEMPERATURE-TIME OF THE FIRE ENVIRONMENT IS
C                         TMPFR4(T), CALCULATED IN THE SUBROUTINE TRTMP4 BY INTERPOLATION/
C                         EXTRAPOLATION OF DATA IN INPUT COMMON BLOCK FIRE4BLK).
C           IBCTYP = 9:   [TMP1IN, TMP1FN] SPECIFIED; THE TEMPERATURE OF SURFACE 1 IS
C                         SPECIFIED AS AS A LINEAR INTERPOLATION IN TIME BETWEEN TMP1IN, AT
C                         TIME TINT, AND TMP1FN, AT TIME TLAST; Q4 SIMULATED TO BE THE HEAT
C                         TRANSFER TO SURFACE 4 FROM AN AMBIENT TEMPERATURE (TAMB)
C                         ENVIRONMENT.
C     IXM
```

```
C               DETERMINES WHETHER XM1(NPTS), XM2(NPTS) IS INPUT OR OUTPUT:
C                       IXM = 1  IF XM1, XM2 ARE TO BE CALCULATED AND THEN PROVIDED AS OUTPUT;
C                       IXM = 2  IF XM1 AND XM2 WERE CALCULATED PREVIOUSLY AND ARE BEING
C                                PROVIDED AS INPUT.
C       NPTS
C               NUMBER OF POINTS IN PANELS WHERE TEMPERATURE IS COMPUTED.
C       NCOND = MCOND
C               NUMBER OF (COND,TEMP) PAIRS USED TO CALCULATE COND VS
C               TEMPERATURE FOR THE GYPSUM PANELS, =< 100.
C       NCP=MCP
C               NUMBER OF (CP,TEMP) PAIRS USED TO CALCULATE CP VS TEMPERATURE FOR THE
C               GYPSUM PANELS, =< 100.
C       NFIRE1
C               NUMBER OF (TEMP, TIME) PAIRS USED TO CALCULATE THE TEMPERATURE-TIME CURVE
C               OF THE FIRE TMPFR1(T) CALCULATED IN THE SUBROUTINE FRTMP1, =< 1000.
C       NFIRE4
C               NUMBER OF (TEMP, TIME) PAIRS USED TO CALCULATE THE TEMPERATURE-TIME CURVE
C               OF THE FIRE TMPFR4(T) CALCULATED IN THE SUBROUTINE FRTMP4, =< 1000.
C       NRHOD = MRHOD
C               NUMBER OF (RHO,TEMP) PAIRS USED TO CALCULATE RHO VS  TEMPERATURE FOR THE
C               GYPSUM PANELS, =< 100.
C       Q1
C               RATE OF HEAT TRANSFER TO SURFACE 1 [W/M**2].
C       Q4
C               RATE OF HEAT TRANSFER TO SURFACE 4 [W/M**2].
C       Q1IN, Q1FN
C               INITIAL, FINAL SPECIFIED Q1 [W/M**2].
C       Q4IN, Q4FN
C               INITIAL, FINAL SPECIFIED Q4 [W/M**2].
C       RHODDATA(1,N)=RHODDAT(1,N), N=1, NRHO = MRHO
C               DENSITY [KG/M**3] OF NTH (DENSITY,TEMP) DATA PAIR USED TOCALCULATE RHO(TEMP)
C               IN SUBROUTINE DSPGYP.
C       RHODDATA(2,N) = RHODDAT(2,N), N=1, NRHO=MRHO
C               TEMP [C] OF  NTH  (DENSITY,TEMP)  DATA  PAIR  USED  TO CALCULATE  RHO(TEMP)  IN
C               SUBROUTINE DSPGYP.
C       SURFACE 1
C               OUTER/LEFT SURFACE OF LEFT PANEL.
C       SURFACE 2
C               INNER/RIGHT SURFACE OF LEFT PANEL.
C       SURFACE 3
C               INNER/LEFT SURFACE OF RIGHT PANEL.
C       SURFACE 4
C               OUTER/RIGHT SURFACE OF RIGHT PANEL.
C       TEMP1
C               TEMPERATURE DISTRIBUTION IN THE LEFT PANEL (I.E., AT THE NPTS POINTS) AT TIME TINT
C               [K].
C       TEMP2
C               TEMPERATURE DISTRIBUTION IN THE RIGHT PANEL (I.E., AT THE NPTS POINTS) AT TIME TINT
C               [K].
C       TINT, TLAST
C               INITAL, FINAL TIMES [S].
C       TMP1IN, TMP1FN
C               INITIAL, FINAL TEMPERATURES OF SURFACE 1 [K].
C       TMP4IN, TMP4FN
C               INITIAL, FINAL TEMPERATURES OF SURFACE 4 [K].
C       TAMB
C               AMBIENT TEMPERATURE OF LABORATORY/OUTSIDE ENVIRONMENT [K]; REQUIRED IF
```

```
C                IBCTYP = 5, 6, 7, OR 9.
C        X
C                DISTANCE FROM LEFT TO RIGHT AS MEASURED FROM SURFACE 1.
C        XM1(N)
C                VALUE OF X IN LEFT PANEL, PANEL 1, AT ITS NTH TEMPERATURE CALCULATED POSITION
C                FROM THE LEFT [I.E., WHERE TEMPERATURE = TEMP1(N) AT TIME TINT], N = 1, NPTS, WHERE
C                THE NPTS ARE EQUALLY SPACED THROUGH HE PANEL THICKNESS [XM1(1) = 0. IS AT
C                SURFACE 1 AND XM1(NPTS) = AL1 IS AT SURFACE 2].
C        XM2(N)
C                VALUE OF X IN RIGHT PANEL, PANEL 2, AT ITS NTH TEMPERATURE-CALCULATED POSITION
C                FROM THE LEFT [I.E., WHERE TEMPERATURE = TEMP2(N) AT TIME TINT], N = 1, NPTS, WHERE
C                THE NPTS ARE EQUALLY SPACED THROUGH THE PANEL THICKNESS [XM2(1) = AL1 + ALGAP
C                IS AT SURFACE 3 AND XM2(NPTS) = AL1 + ALGAP + AL2 IS AT SURFACE 4].
C
C        INPUT (IN ORDER OF CALL TO THIS SUBROUTINE):
C        1)      AT TIME=TINT: TEMP1(N), TEMP2(N), N = 1, NPTS;
C        2)      IXM;
C        3)      XM1(N), XM2(N), N = 1, NPTS; ONLY REQUIRED IF IXM > 1;
C        4)      NPTS;
C        5)      IBCTYP;
C        6)      EPS1,EPS2,EPS3,AND EPS4;
C        7)      EPSFUR; ONLY REQUIRED IF IBCTYPE=5, 6, 7, OR 8;
C        8)      EPSCAL;
C        9)      TINT, TLAST;
C        10)     TMP1IN; ONLY REQUIRED IF IBCTYP = 3, 4, OR 9;
C        11)     TMP4IN; ONLY REQUIRED IF IBCTYP = 2 OR 4;
C        12)     TMP1FN; ONLY REQUIRED IF IBCTYP = 3, 4, OR 9;
C        13)     TMP4FN; ONLY REQUIRED IF IBCTYP = 2 OR 4;
C        14)     TAMB; ONLY REQUIRED IF IBCTYP = 5, 6, 7, OR 9;
C        15)     Q1IN, Q1FN; ONLY REQUIRED IF IBCTYP = 1 OR 2;
C        16)     Q4IN, Q4FN; ONLY REQUIRED IF IBCTYP = 1 OR 3;
C        17)     AL1, AL2, ALGAP;
C        18)     DENAMB;
C        19)     MRHOD,RHODDAT(2,MRHOD),MCP,CPDAT(2,MCP),MCOND,
C                CONDDAT(2,MCOND); MRHOD =< 100, MCP =< 100, MCOND =< 100;
C        20)     COMMON/FIRE1/NFIRE1,FIRE1DAT(2,1000), ONLY REQUIRED IF
C                IBCTYP = 7 OR 8; NFIRE1 =< 1000;
C        21)     COMMON/FIRE4/NFIRE4,FIRE4DAT(2,1000), ONLY REQUIRED IF
C                IBCTYP = 8; NFIRE4 =< 1000.
C
C        OUTPUT:
C        1)      XM1(N), XM2(N), N = 1, NPTS;
C        2)      AT TIME=TLAST:
C                A)      TEMP1(N), TEMP2(N), N = 1, NPTS;
C                B)      Q1FN = Q1, THIS IS ONLY COMPUTED IF IBCTYP = 3,
C                        4, 5, 6, 7, OR 8;
C                C)      Q4FN = Q4, THIS IS ONLY COMPUTED IF IBCTYP = 2,
C                        4, 5, 6, 7, 8, OR 9.
C
C*************************************************************************
C*************************************************************************
```

TABLE 1. Parameters of the 1x1 and 1x2 assemblies/tests and their *GYPST* simulations.

	1x1 assembly/test	1x2 assembly/test
Assembly/test parameters:		
T_{AMB}	23 °C	26 °C
Properties of gypsum:		
ρ(20 °C)	698 kg/m^3	
$\rho(T)/\rho(T = 20\ °C)$, $C_p(T)$, and $k(T)$	from APPENDIX A	
L_1	0.0159 m	0.0127 m
L_2	0.0159 m	0.0254 m
L_{GAP}	0.0900 m	
Additional *GYPST* input parameters:		
IBCTYP	5	
EPSCAL	10^{-5}, 10^{-4}, 10^{-3}, 10^{-2}, 10^{-1}	10^{-5}
ε_i, i = 1 - 4	0.9, 0.8, 0.7, or 0.5	
ε_{FUR}	0.9, 0.8, or 0.7	
NPTS	10 or 20	11 or 21

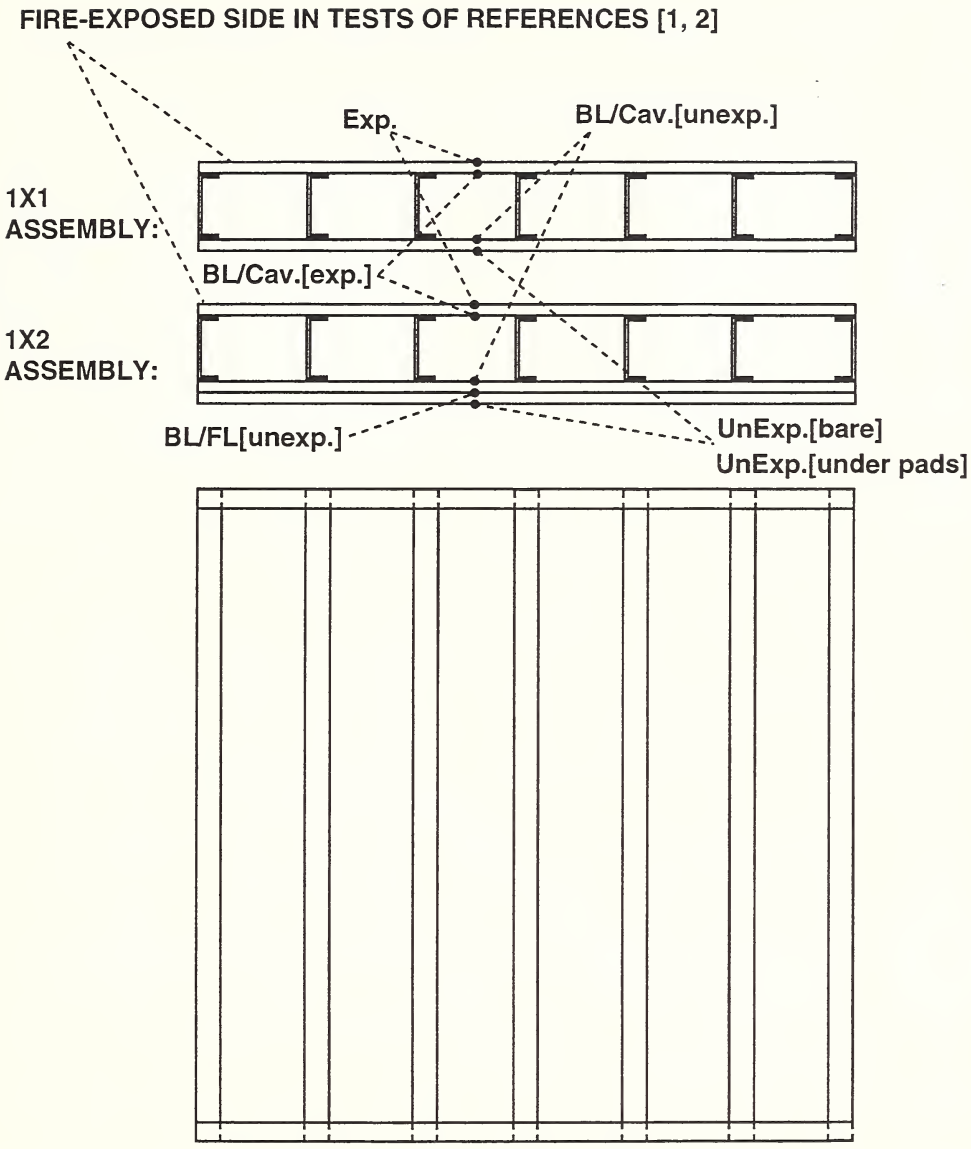

Figure 1. Sketch of example wall system designs (adopted from References [1] and [2]); locations of calculated/measured temperatures in tests of [1] and [2].

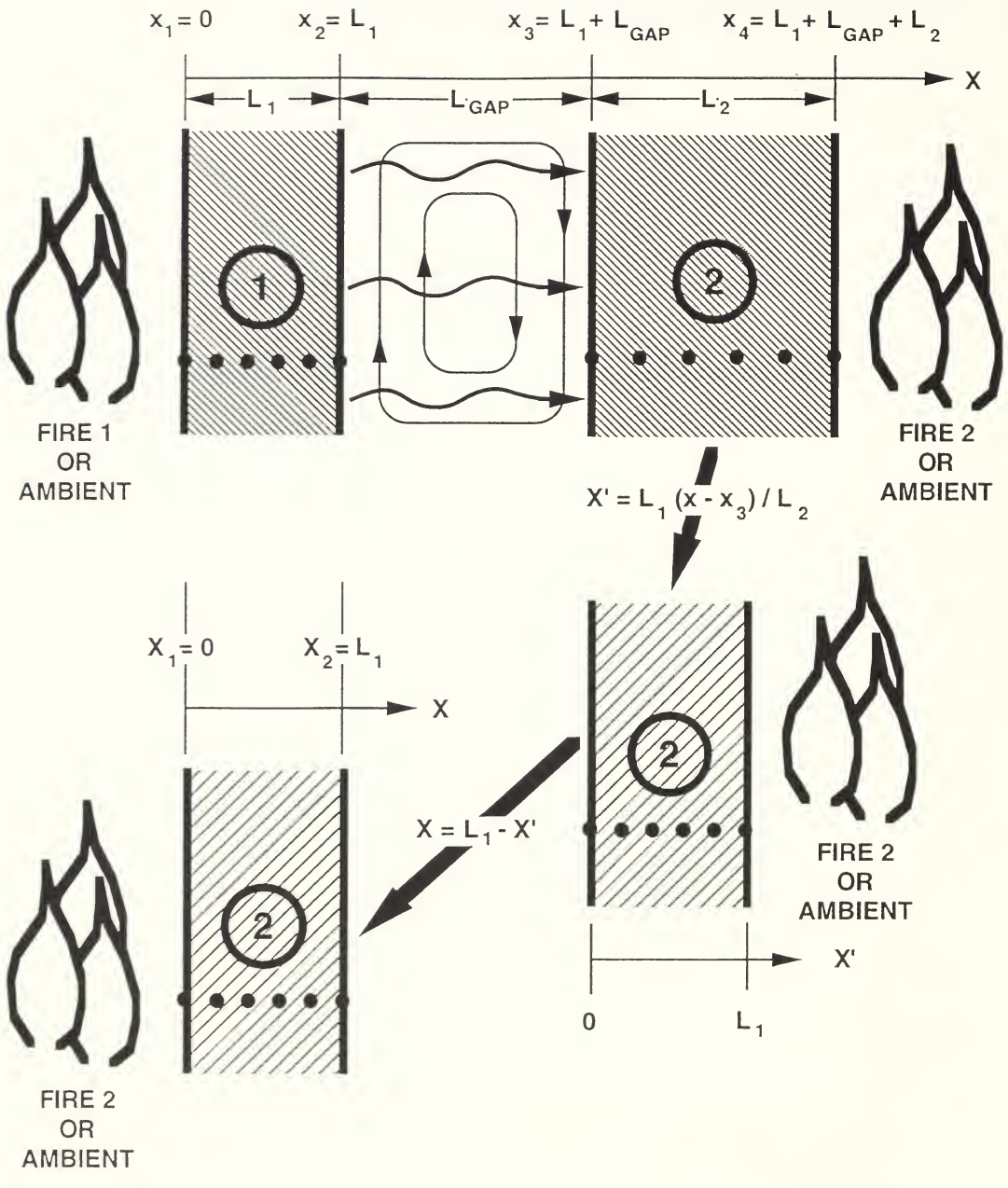

Figure 2. Geometry of the arbitrary two-panel wall system and a depiction of the $x \Rightarrow X$ transformation of Eq. (22).

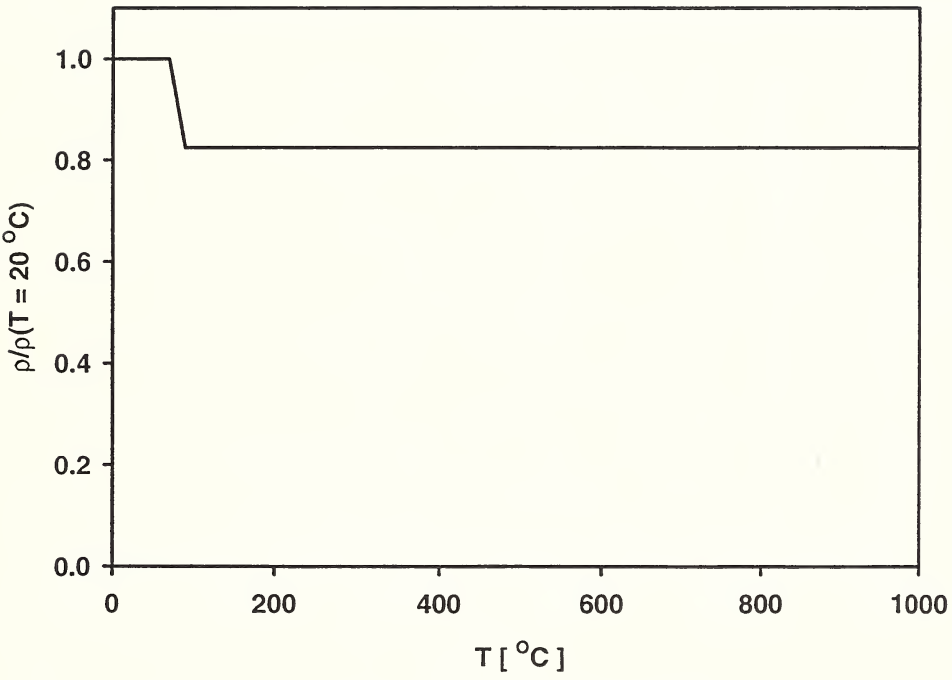

Figure 3. **ρ(T)/ρ(T = 20 °C) representation of APPENDIX A, Eq. (A-2) used for the wall-response simulations.**

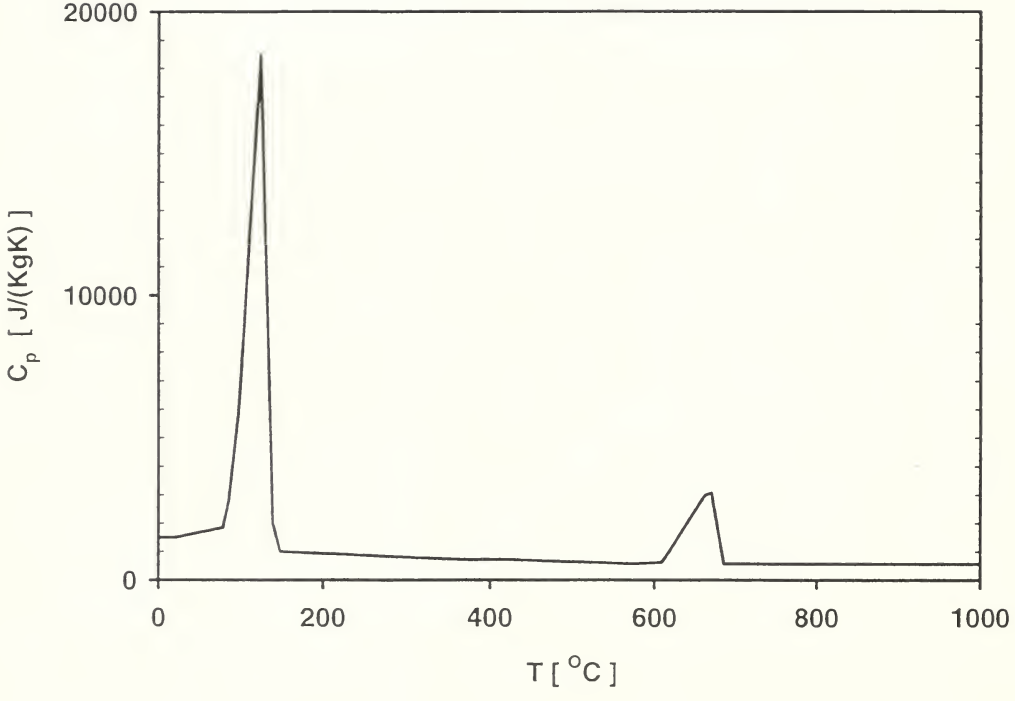

Figure 4. $C_p(T)$ representation of APPENDIX A, Eq. (A-3) used for the wall-response simulations.

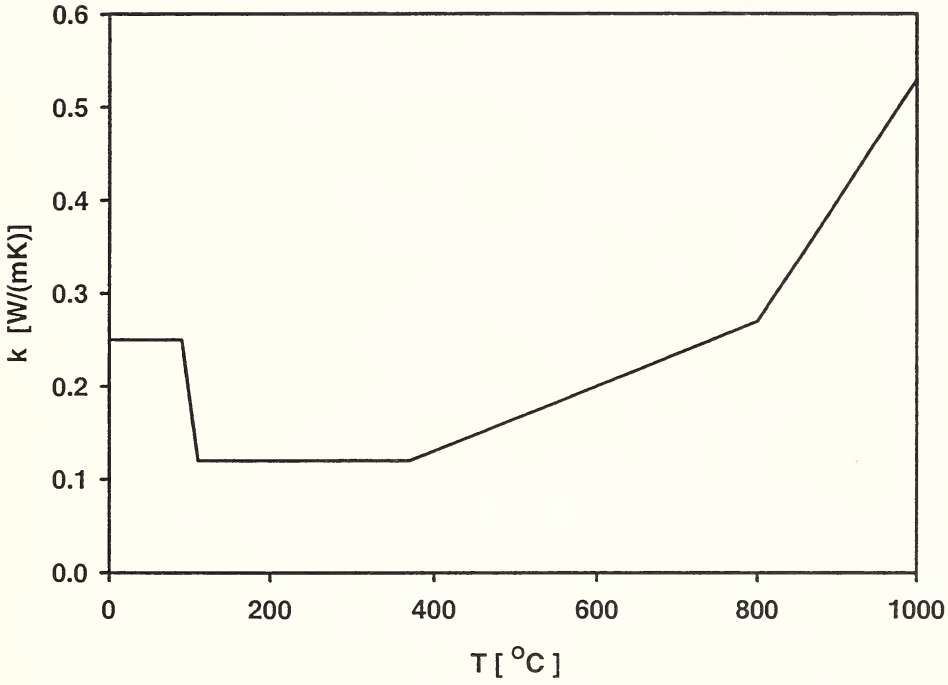

Figure 5. k(T) representation of APPENDIX A, Eq. (A-4) used for the wall-response simulations.

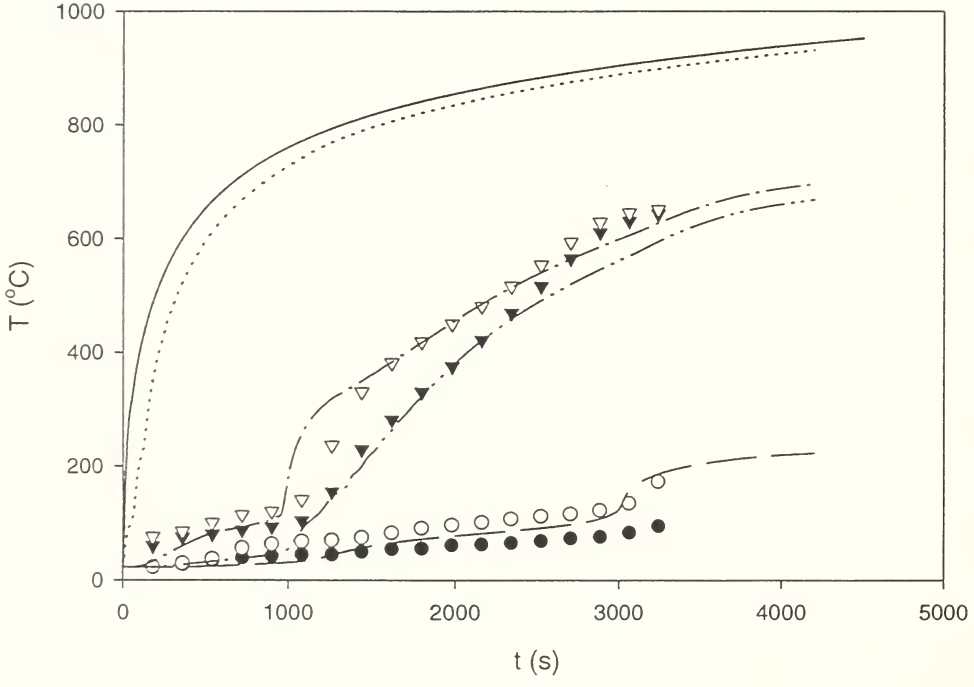

(a) Simulation parameters: NPTS = 20; EPSCAL = 0.00001; ε_{FUR} = all ε_i = 0.9

Figure 6. 1x1 assembly/test: simulated and averaged measured temperatures.

T_{STD} _____; Exp. .....(calc); BL/Cav.[exp.] _.__.__.(calc), ▽▽▽(meas.); BL/Cav.[unexp.] _.__.__.(calc), ▼▼▼(meas); UnExp. __ __ (calc); UnExp.[under pads] ○○○(meas); UnExp.[bare] ●●●.

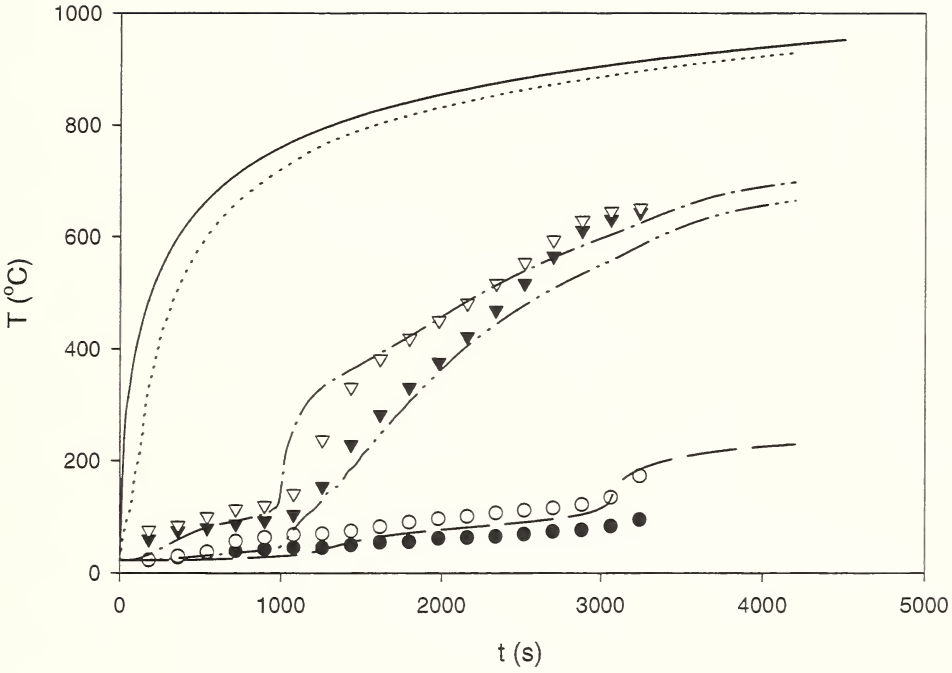

(b) Simulation parameters: NPTS = 20; EPSCAL = 0.00001; ε_{FUR} = all ε_i = 0.8

Figure 6. **1x1 assembly/test: simulated and averaged measured temperatures.**

(Cont'd) **T_{STD} _____; Exp. .....(calc); BL/Cav.[exp.] .__.__.(calc), ▽▽▽(meas.); BL/Cav.[unexp.] ..__..__..(calc), ▼▼▼(meas); UnExp. __ __ (calc); UnExp.[under pads] ○○○(meas); UnExp.[bare] ●●●.**

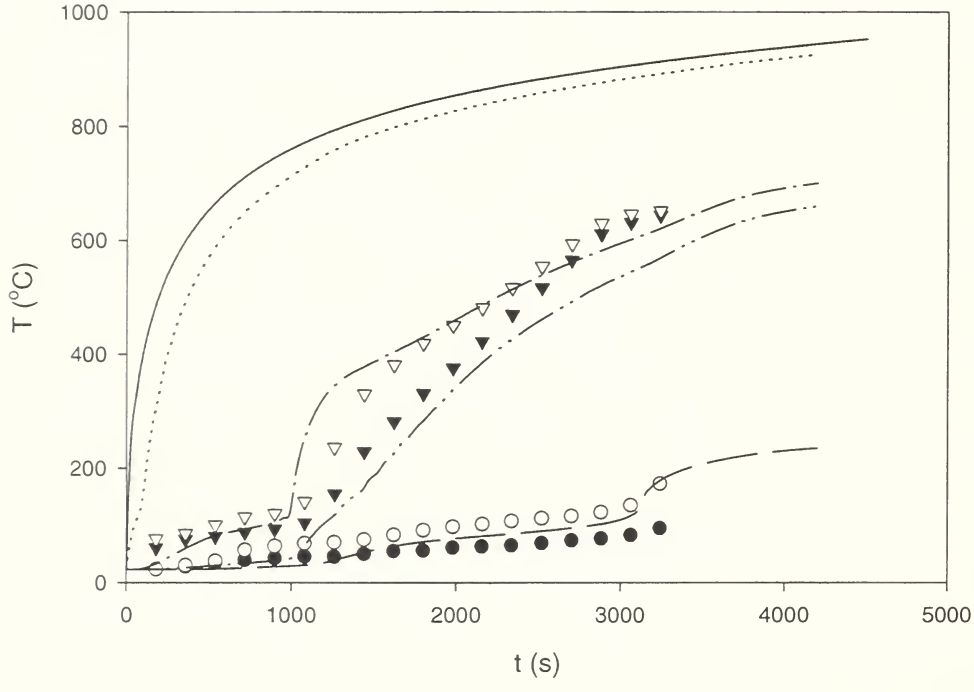

(c) Simulation parameters: NPTS = 20; EPSCAL = 0.00001; ε_{FUR} = all ε_i = 0.7

Figure 6. 1x1 assembly/test: simulated and averaged measured temperatures.

(Cont'd) T_{STD} _____; Exp. .....(calc); BL/Cav.[exp.] _.__.__.(calc), ▽▽▽(meas.); BL/Cav.[unexp.] _..__..__..(calc), ▼▼▼(meas); UnExp. __ __ (calc); UnExp.[under pads] ○○○(meas); UnExp.[bare] ●●●.

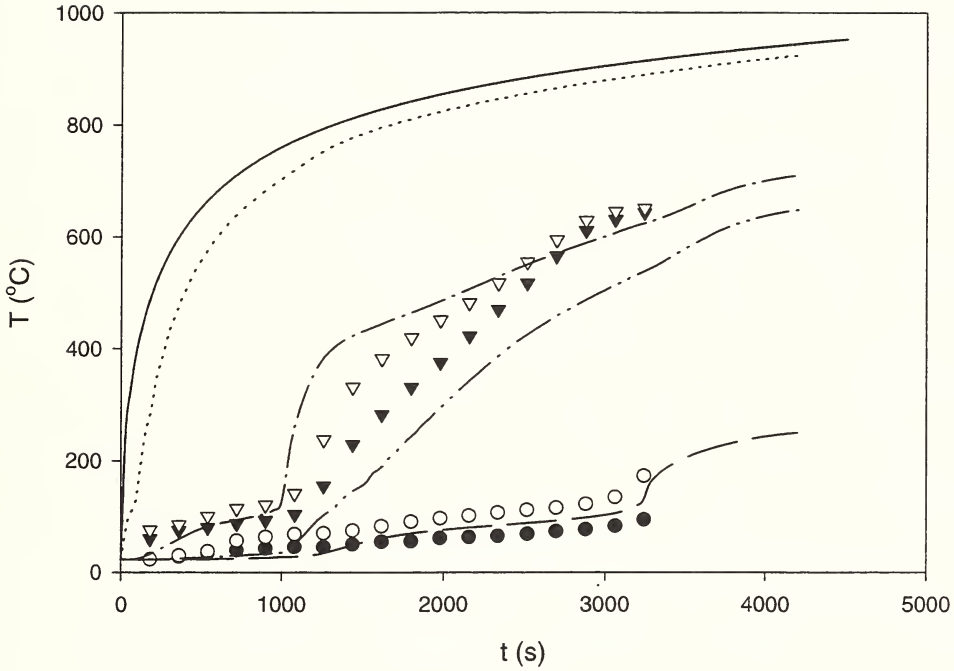

(d) Simulation parameters: NPTS = 20; EPSCAL = 0.00001; $\varepsilon_{FUR} = 0.8$, all $\varepsilon_i = 0.5$

Figure 6. **1x1 assembly/test: simulated and averaged measured temperatures.**

(Cont'd) **T_{STD} _____; Exp. .....(calc); BL/Cav.[exp.] ._._._(calc), ▽▽▽(meas.); BL/Cav.[unexp.] .._._._..(calc), ▼▼▼(meas); UnExp. __ __ (calc); UnExp.[under pads] ○○○(meas); UnExp.[bare] ●●●.**

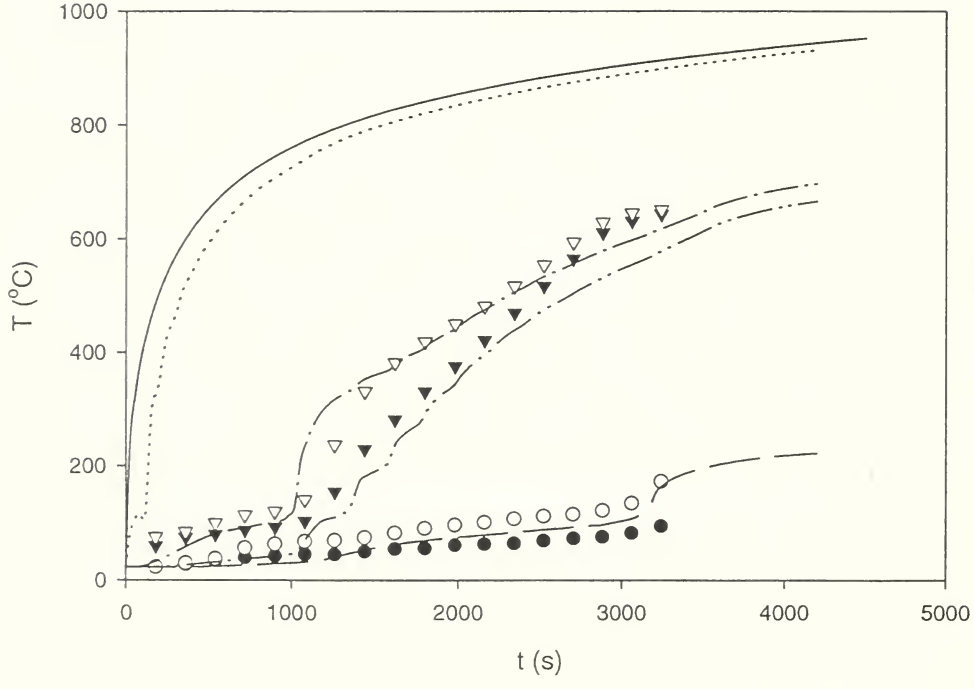

Figure 7. 1x1assembly/test: simulated [NPTS = 10; EPSCAL = 0.00001; ε_{FUR} = all ε_i = 0.9] and averaged measured temperatures. T_{STD} _____;

Exp. .....(calc); BL/Cav.[exp.] .__.__.(calc), ▽▽▽(meas.); BL/Cav.[unexp.] ..__..__..(calc), ▼▼▼(meas); UnExp. __ __ (calc); UnExp.[under pads] ○○○(meas); UnExp.[bare] ●●●.

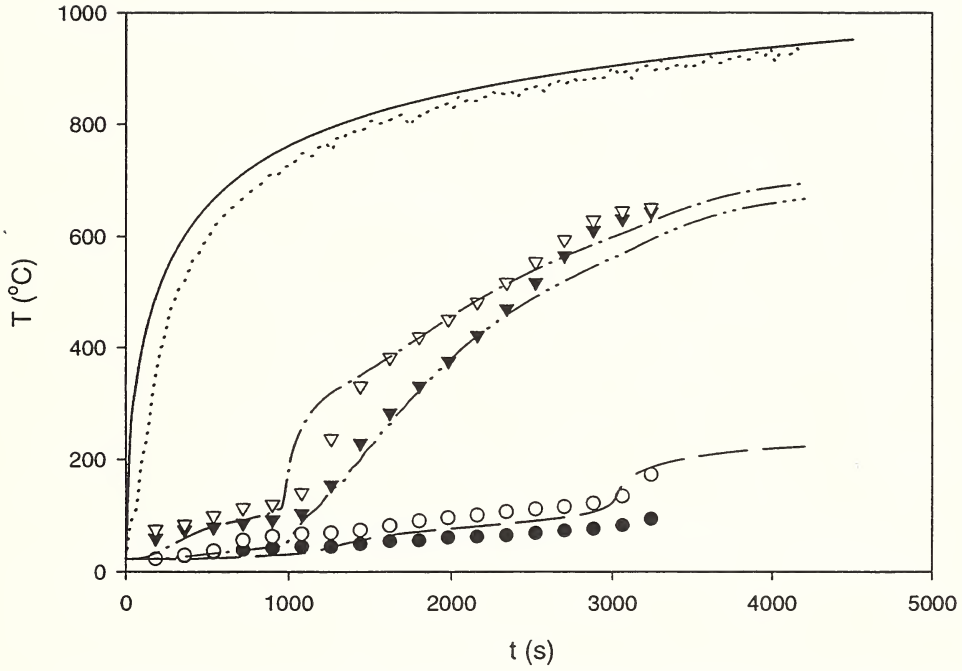

Figure 8. **1x1assembly/test: simulated [NPTS = 20; EPSCAL = 0.01; ε_{FUR} = all ε_i = 0.9] and averaged measured temperatures. T_{STD} _____; Exp. .....(calc); BL/Cav.[exp.] .___.___.(calc), ▽▽▽(meas.); BL/Cav.[unexp.] ..___..___..(calc), ▼▼▼(meas); UnExp. __ __ (calc); UnExp.[under pads] ○○○(meas); UnExp.[bare] ●●●.**

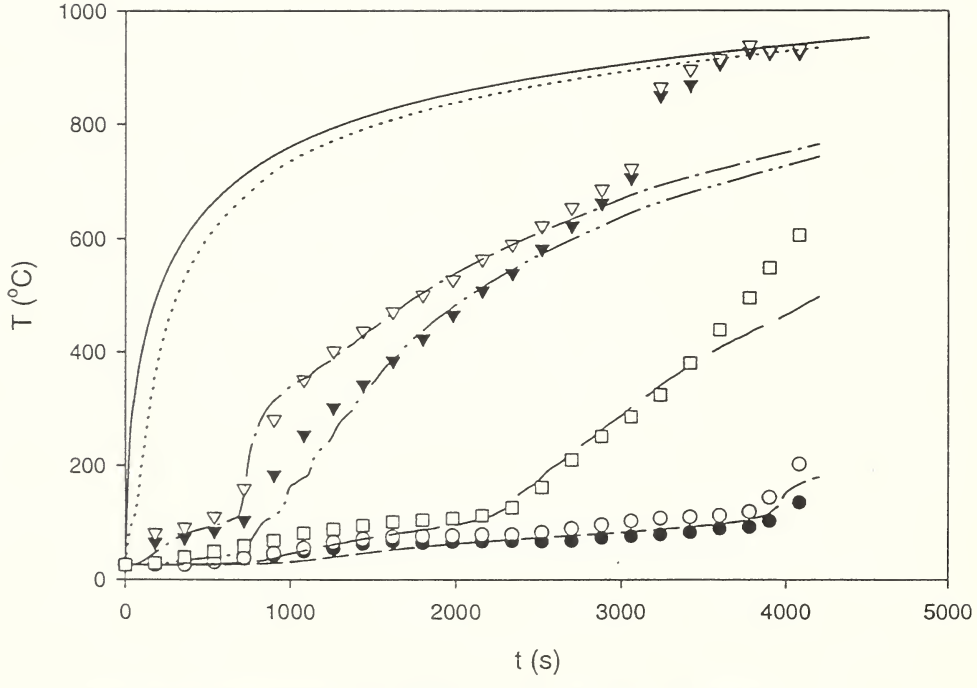

(a) Simulation parameters: NPTS = 21; EPSCAL = 0.00001; ε_{FUR} = all ε_i = 0.9

Figure 9. 1x2 assembly/test: simulated and averaged measured temperatures. T_{STD} _____; Exp. .....(calc); BL/Cav.[exp.] _.__.__.(calc), ▽▽▽(meas.); BL/Cav.[unexp.] _.__.__.(calc), ▼▼▼(meas); UnExp. __ __ (calc); BL/FL[unexp.] ____ ____ (calc), □□□ (meas); UnExp.[under pads] ○○○(meas); UnExp.[bare] ●●●.

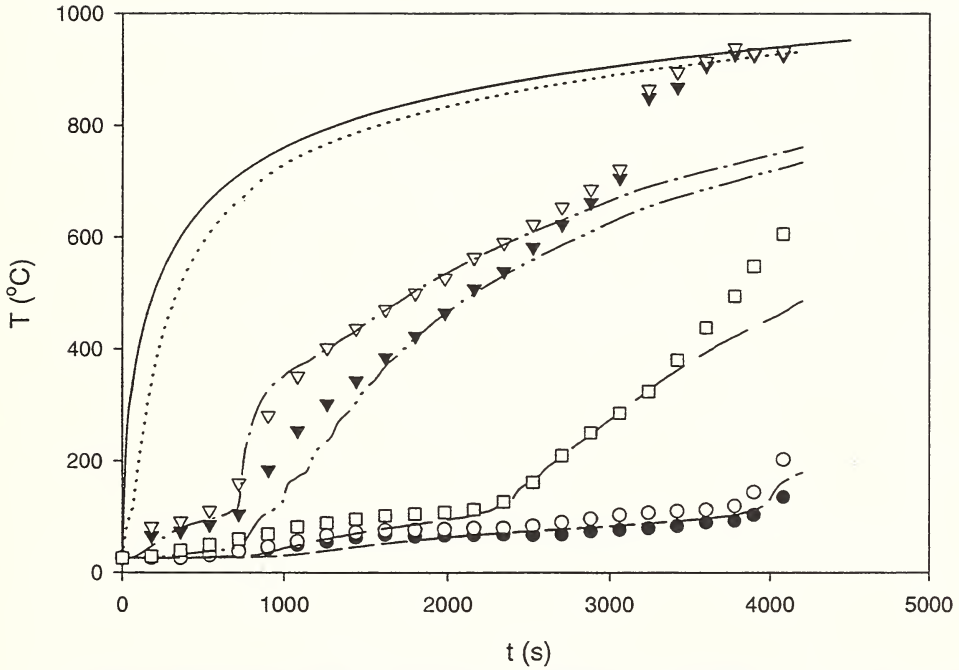

(b) Simulation parameters: NPTS = 21; EPSCAL = 0.00001; ε_{FUR} = all ε_i = 0.8

Figure 9. (Cont'd) 1x2 assembly/test: simulated and averaged measured temperatures. T_{STD} _____; Exp. .....(calc); BL/Cav.[exp.] _.__.__.(calc), ▽▽▽(meas.); BL/Cav.[unexp.] _..__..__..(calc), ▼▼▼(meas); UnExp. __ __ (calc); BL/FL[unexp.] ____ ____ (calc), □□□ (meas); UnExp.[under pads] ○○○(meas); UnExp.[bare] ●●●.

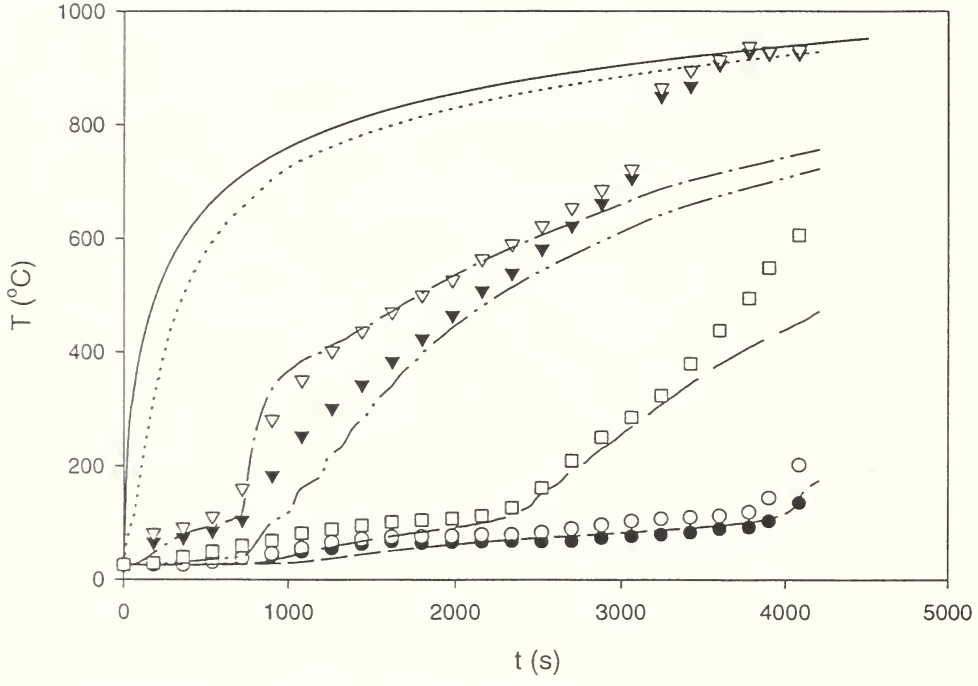

(c) Simulation parameters: NPTS = 21; EPSCAL = 0.00001; ε_{FUR} = all ε_i = 0.7

Figure 9. (Cont'd) 1x2 assembly/test: simulated and averaged measured temperatures. T_{STD} _____; Exp. .....(calc); BL/Cav.[exp.] _ _ _(calc), ▽▽▽(meas.); BL/Cav.[unexp.] _ _ _(calc), ▼▼▼(meas); UnExp. __ __ (calc); BL/FL[unexp.] ____ ____ (calc), □□□ (meas); UnExp.[under pads] ○○○(meas); UnExp.[bare] ●●●.

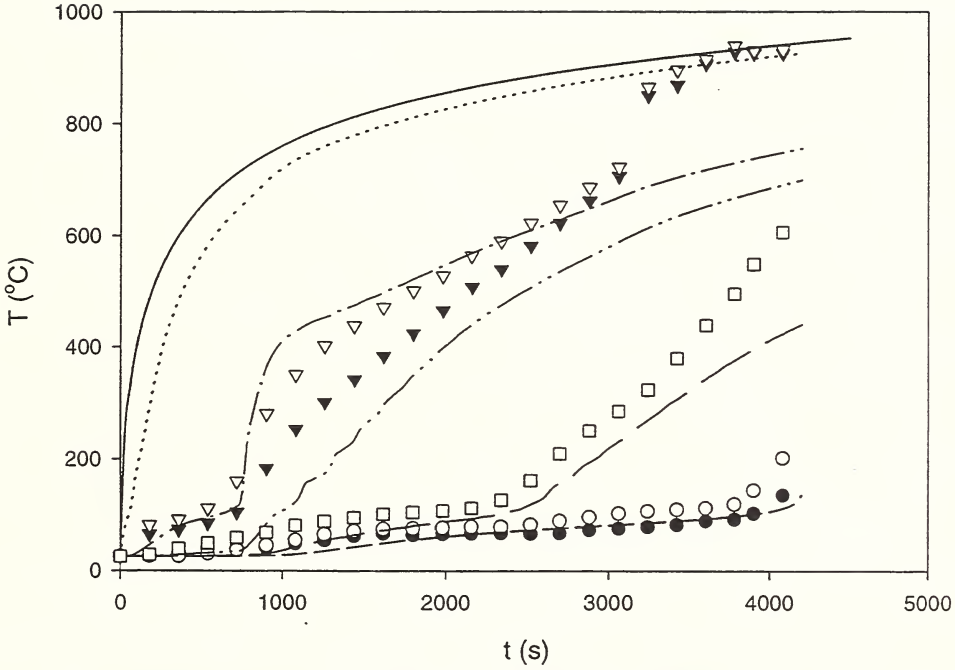

(d) Simulation parameters: NPTS = 21; EPSCAL = 0.00001; $\varepsilon_{FUR} = 0.8$, all $\varepsilon_i = 0.5$

Figure 9. 1x2 assembly/test: simulated and averaged measured temperatures.

(Cont'd) T_{STD} _____; Exp. .....(calc); BL/Cav.[exp.] _.__.__.(calc), ▽▽▽(meas.); BL/Cav.[unexp.] _.__.__.(calc), ▼▼▼(meas); UnExp. __ __ (calc); BL/FL[unexp.] ____ ____ (calc), □□□ (meas); UnExp.[under pads] ○○○(meas); UnExp.[bare] ●●●.

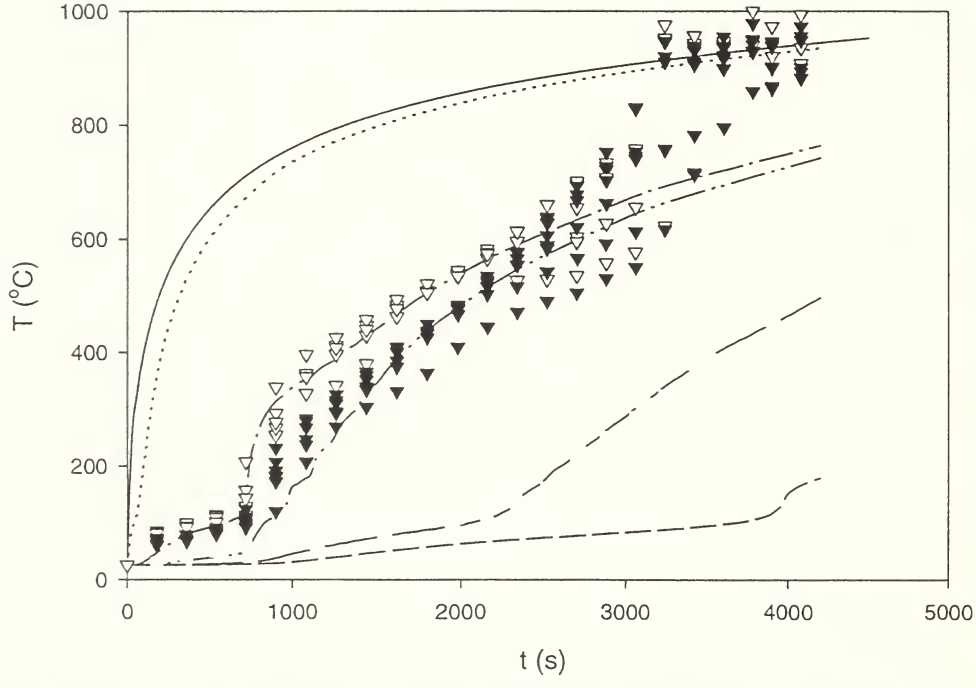

Figure 10. 1x2 assembly/test: simulated [NPTS = 21; EPSCAL = 0.00001; ε_{FUR} = all ε_i = 0.9] and individual measured temperatures at BL/Cav.[exp.] and BL/Cav.[unexp.].

T_{STD} _____; Exp. .....(calc); BL/Cav.[exp.] _._._.(calc), ▽▽▽(meas.); BL/Cav.[unexp.] _.._.._..(calc), ▼▼▼(meas); BL/FL[unexp.] ____ ____ (calc); UnExp. __ __ (calc).

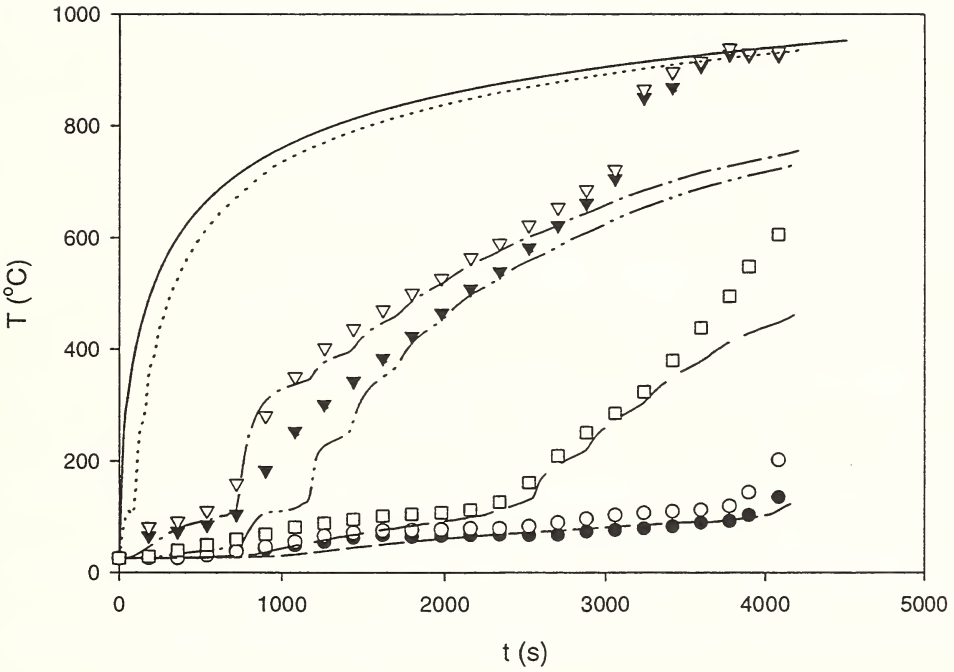

Figure 11. **1x2 assembly/test: simulated [NPTS = 11; EPSCAL = 0.00001; ε_{FUR} = all ε_i = 0.9] and averaged measured temperatures. T_{STD} _____;**

Exp. .....(calc); BL/Cav.[exp.] _._._.(calc), ▽▽▽(meas.); BL/Cav.[unexp.] _.._.._..(calc), ▼▼▼(meas); BL/FL[unexp.] ____ ____ (calc), □□□ (meas); UnExp. __ __ (calc); UnExp.[under pads] ○○○(meas); UnExp.[bare] ●●●.

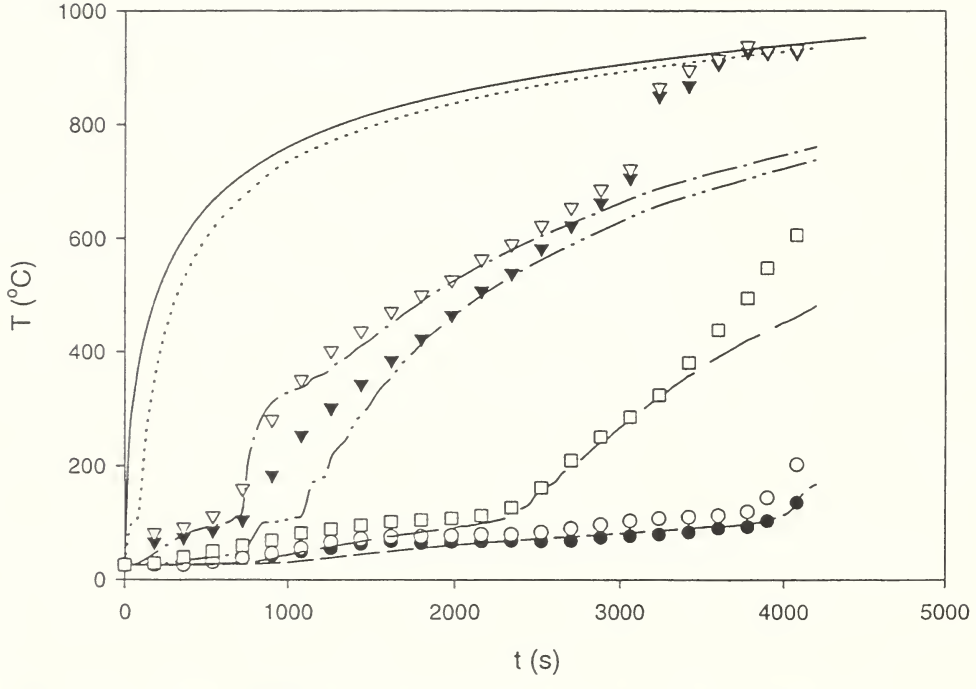

Figure 12. 1x2 assembly/test: simulated [with "nearly"-discontinuous ρ(T) and k(T); NPTS = 21; EPSCAL = 0.00001; ε_{FUR} = all ε_i = 0.9] and averaged measured temperatures. T_{STD} _____; Exp. .....(calc);

BL/Cav.[exp.] _.__.__.(calc), ▽▽▽(meas.);
BL/Cav.[unexp.] ..__..__..(calc), ▼▼▼(meas);
BL/FL[unexp.] ____ ____ (calc), □□□ (meas); UnExp. __ __ (calc);
UnExp.[under pads] ○○○(meas); UnExp.[bare] ●●●.

NIST-114
(REV. 6-93)
ADMAN 4.09

U.S. DEPARTMENT OF COMMERCE
NATIONAL INSTITUTE OF STANDARDS AND TECHNOLOGY

MANUSCRIPT REVIEW AND APPROVAL

(ERB USE ONLY)
ERB CONTROL NUMBER | DIVISION
PUBLICATION REPORT NUMBER: NISTIR 6027 | CATEGORY CODE
PUBLICATION DATE: June 1997 | NUMBER PRINTED PAGES

INSTRUCTIONS: ATTACH ORIGINAL OF THIS FORM TO ONE (1) COPY OF MANUSCRIPT AND SEND TO THE SECRETARY, APPROPRIATE EDITORIAL REVIEW BOARD

TITLE AND SUBTITLE (CITE IN FULL)

THE THERMAL RESPONSE OF GYPSUM-PANEL/STEEL-STUD WALL SYSTEMS EXPOSED TO FIRE ENVIRONMENTS - A SIMULATION FOR USE IN ZONE-TYPE FIRE MODELS

CONTRACT OR GRANT NUMBER | TYPE OF REPORT AND/OR PERIOD COVERED

AUTHOR(S) (LAST NAME, FIRST INITIAL, SECOND INITIAL)

Cooper, Leonard Y.

PERFORMING ORGANIZATION (CHECK (X) ONE BOX)
[x] NIST/GAITHERSBURG
[ ] NIST/BOULDER
[ ] JILA/BOULDER

LABORATORY AND DIVISION NAMES (FIRST NIST AUTHOR ONLY)
Building and Fire Research Laboratory

SPONSORING ORGANIZATION NAME AND COMPLETE ADDRESS (STREET, CITY, STATE, ZIP)

PROPOSED FOR NIST PUBLICATION

[ ] JOURNAL OF RESEARCH (NIST JRES)	[ ] MONOGRAPH (NIST MN)	[ ] LETTER CIRCULAR
[ ] J. PHYS. & CHEM. REF. DATA (JPCRD)	[ ] NATL. STD. REF. DATA SERIES (NIST NSRDS)	[ ] BUILDING SCIENCE SERIES
[ ] HANDBOOK (NIST HB)	[ ] FEDERAL INF. PROCESS. STDS. (NIST FIPS)	[ ] PRODUCT STANDARDS
[ ] SPECIAL PUBLICATION (NIST SP)	[ ] LIST OF PUBLICATIONS (NIST LP)	[ ] OTHER _____
[ ] TECHNICAL NOTE (NIST TN)	[x] NIST INTERAGENCY/INTERNAL REPORT (NISTIR)	

PROPOSED FOR NON-NIST PUBLICATION (CITE FULLY) [x] U.S. [ ] FOREIGN

PUBLISHING MEDIUM
[x] PAPER [ ] CD-ROM
[ ] DISKETTE (SPECIFY) _____
[ ] OTHER (SPECIFY)

SUPPLEMENTARY NOTES

ABSTRACT (A 2000-CHARACTER OR LESS FACTUAL SUMMARY OF MOST SIGNIFICANT INFORMATION. IF DOCUMENT INCLUDES A SIGNIFICANT BIBLIOGRAPHY OR LITERATURE SURVEY, CITE IT HERE. SPELL OUT ACRONYMS ON FIRST REFERENCE.) (CONTINUE ON SEPARATE PAGE, IF NECESSARY.)

This work develops a method for simulating the thermal response of fire-environment-exposed wall systems constructed of arbitrary-thickness gypsum panels mounted on either side of vertical steel studs. The studs, separated at regular intervals, form an unfilled air gap between the panels

The main objective is an experimentally-validated, modular, thermal-wall-model algorithm that can be easily integrated into zone-type compartment fire models and that can be used in "stand-alone" analyses.

The algorithm solves an initial-value/boundary-value problem for the temperature distribution through the thicknessess of the two panels and within a specified time interval. The analysis is based on temperature-dependent thermal properties for the gypsum. The initial temperature distribution and the type of boundary conditions at the outer surfaces are user-specified. A variety of choices for the boundary conditions are available. These include boundary conditions that are expected to satisfy the requirements of any zone-type fire model and those that can be used to determine fire performance of the wall systems in ASTM E119 or ISO 834 tests. The algorithm output includes the final temperature distribution and, when outer surface temperatures are specified, the final rate of heat transfer to these surfaces.

KEY WORDS (MAXIMUM OF 9; 28 CHARACTERS AND SPACES EACH; SEPARATE WITH SEMICOLONS; ALPHABETIC ORDER; CAPITALIZE ONLY PROPER NAMES)
Algorithms, ASTM E119, compartment fires, fire barriers, fire models, gypsum board, steel studs, walls, zone models

AVAILABILITY
[x] UNLIMITED [ ] FOR OFFICIAL DISTRIBUTION - DO NOT RELEASE TO NTIS
[ ] ORDER FROM SUPERINTENDENT OF DOCUMENTS, U.S. GPO, WASHINGTON, DC 20402
[x] ORDER FROM NTIS, SPRINGFIELD, VA 22161

NOTE TO AUTHOR(S): IF YOU DO NOT WISH THIS MANUSCRIPT ANNOUNCED BEFORE PUBLICATION, PLEASE CHECK HERE. [ ]

WORDPERFECT